FATİH SULTAN MEHMET VAKIF ÜNİVERSİTESİ
LİSANSÜSTÜ EĞİTİM ENSTİTÜSÜ
BİYOMEDİKAL MÜHENDİSLİĞİ ANABİLİM DALI
BİYOMEDİKAL MÜHENDİSLİĞİ PROGRAMI

DEEP LEARNING METHODS FOR CLASSIFICATION ALZHEIMER'S DISEASE

YÜKSEK LİSANS TEZİ

HUSAM MOHAMMED ABDULFATTAH SAIF AL-HAMMADI

İSTANBUL, 2023

FATİH SULTAN MEHMET VAKIF ÜNİVERSİTESİ
LİSANSÜSTÜ EĞİTİM ENSTİTÜSÜ
BİYOMEDİKAL MÜHENDİSLİĞİ ANABİLİM DALI
BİYOMEDİKAL MÜHENDİSLİĞİ PROGRAMI

DEEP LEARNING METHODS FOR CLASSIFICATION ALZHEIMER'S DISEASE

YÜKSEK LİSANS TEZİ

HUSAM MOHAMMED ABDULFATTAH SAIF AL-HAMMADI
(YU190231102)

Danışman
(Dr. Öğr. Üyesi Ebubekir Koç)

İSTANBUL, 2023

FATİH SULTAN MEHMET VAKIF ÜNİVERSİTESİ
TEZ ONAY FORMU

23/06/2023

LİSANSÜSTÜ EĞİTİM ENSTİTÜSÜ MÜDÜRLÜĞÜNE

Biyomedikal Mühendisliği Anabilim Dalı Biyomedikal Mühendisliği tezli yüksek lisans programı öğrencisi YU190231102 numaralı ***Husam Mohammed Abdulfattah Saif Al-HAMMADI*** nın, hazırladığı *"ANN Yöntemi İle Normal ve Anormal (Alzheimer Hastalığı) EEG Tespiti"* konulu Yüksek Lisans tezi ile ilgili Tez Savunma Sınavı, 23.06.2023 Cuma günü saat 11:00'da yapılmış, sorulara alınan cevaplar sonunda adayın tezinin **Kabulüne Oy Çokluğu/Oy Birliği** ile karar verilmiştir.

Tez adı değişikliği yapılması halinde: Tez adının
"**Alzheimer Hastalığının Sınıflandırılmasına Yönelik Derin Öğrenme Yöntemleri"**
şeklinde değiştirilmesi uygundur.

	Jüri Üyesi	**Karar**
1.	(Danışman) Dr. Öğr. Üyesi Ebubekir KOÇ	Kabul
2.	Dr. Öğr. Üyesi Hayriye AKTAŞ DİNÇER	Kabul
3.	Dr. Öğr. Üyesi Süha TUNA	Kabul
4.	.....	.....
5.	.....	.....
6.	(İkinci Danışman)*.....	.....

**2. Danışman varsa doldurulması gerekmektedir.*

DECLARATION

I declare that scientific ethics were followed in the writing of this thesis, that the works of others are referred to in accordance with scientific norms in case of use, no falsification has been made in the data used, and no part of the thesis has been presented as another study at my university or another university.

Husam Al-Hammadi

ACKNOWLEDGMENT

First and foremost, all thankfulness to Allah, the Beneficent, the Merciful, the One, on who all depend, and none is like Him. Allah, who helps and guides me to overcome the challenges during my study and my life,

Sincere gratitude and many thanks must be expressed to:

My supervisor Dr. Öğr. Üyesi Ebubekir KOÇ who is a tremendous mentor for me, for his constructive criticism, experienced guidance, hours of discussions and patience with which he checked and corrected many technical errors during the preparation of this work.

Dr. Ahmet Yıldrım from the EEG department at Kartal Dr. Lütfi Kirdar hospital for guiding the EEG signals' diagnosis.

I am extremely thankful to Turkiye Scholarships (YTB) for offering me the opportunity to study in beautiful Turkiye. Moreover, I would also like to dedicate this work to my family who support, encourage, and motivate me. I warmly thank my wife for helping me out in time of need. I will not forget all the other friends that had accompanied me, through thick and thin. they have supported me when time are of essence.

DEEP LEARNING METHODS FOR CLASSIFICATION ALZHEIMER'S DISEASE

Husam Al-Hammadi

ABSTRACT:

Alzheimer's disease (AD) is a progressive and irreversible brain disorder that affects memory, thinking, and behavior. It is the leading cause of dementia. Early diagnosis can slow the progression of Alzheimer's disease and improve the prognosis and increase the quality and quantity of patient care. One of the primary methods in early diagnosis is electroencephalography (EEG), which has been indicated as a promising method for detecting aberrant brain patterns associated to Alzheimer's disease in aspects of low cost, noninvasive, and portability. Furthermore, artificial intelligence tools have been essential in developing models that facilitate disease diagnosis and detection. Deep learning is a promising approach for such applications; however, it requires a reliable dataset. Due to the patient's rights, researchers may not be able to access a sufficient dataset to train the network. This work aims to propose a model to address this issue. Frist, Generative Adversarial Networks (GNN) model is presented to generate an artificial EEG dataset for Alzheimer's disease. It may be employed to understand brain processes better and make more accurate medical diagnoses for Alzheimer's disease using deep learning tools. Then four models have been focused on, Convolutional neural Network (CNN), Recurrent Neural Network (RNN), Multi-layer perceptron (MLP) and Transformer, to classify the Alzheimer's EEG signals. The results show that the GNN model can generate reliable artificial EEG signals for Alzheimer's disease in related channels. Moreover, the proposed models achieve accurate classification with a high accuracy 99.98 %, 99.76 %, 97.58 %, and 97.34 % respectively. Our study has demonstrated that the proposed methodologies serve as a promising complementary tool for identifying potential biomarkers that can aid in the clinical diagnosis of Alzheimer's disease.

Keywords: Alzheimer's Disease, Electroencephalography (EEG), Generative Adversarial Network (GAN), Convolutional neural Network (CNN), Recurrent Neural Network (RNN), Multi-layer perceptron (MLP), and Transformer.

ALZHEIMER HASTALIĞININ SINIFLANDIRILMASINA YÖNELİK DERİN ÖĞRENME YÖNTEMLERİ

Husam Al-Hammadı

ÖZET

Alzheimer hastalığı (AD), hafızayı, düşünmeyi ve davranışı etkileyen ilerleyici ve geri döndürülemez bir beyin bozukluğudur. Bunaklığın önde gelen nedenidir. Erken teşhis, Alzheimer hastalığının ilerlemesini yavaşlatabilir, prognozu iyileştirebilir ve hasta bakımının nitelik ve niceliğini artırabilir. Erken tanıda birincil yöntemlerden biri; düşük maliyetli, invazif olmayan ve taşınabilirlik açılarından Alzheimer hastalığı ile ilişkili anormal beyin modellerini saptamak için umut verici bir yöntem olarak belirtilen elektroensefalografidir (EEG). Ayrıca, yapay zeka araçları, hastalık teşhisini ve tespitini kolaylaştıran modellerin geliştirilmesinde de önemli olmuştur. Derin öğrenme, bu tür uygulamalar için gelecek vaat eden bir yaklaşımdır; ancak güvenilir bir veri seti gerektirir. Hasta hakları nedeniyle, araştırmacılar ağı eğitmek için yeterli bir veri setine erişemeyebilirler. Bu çalışma, bu sorunu çözmek için bir model önermeyi amaçlamaktadır. İlk olarak, Alzheimer hastalığı için yapay bir EEG veri seti oluşturmak üzere, Üretken Çekişmeli Ağlar (GNN) modeli sunulmuştur. Beyin süreçlerini daha iyi anlamak ve derin öğrenme araçlarını kullanarak Alzheimer hastalığı için daha doğru tıbbi teşhis yapmak için kullanılabilir. Daha sonra Alzheimer EEG sinyallerini sınıflandırmak için Evrişimli Sinirsel Ağı (CNN), Devirli Sinirsel Ağı (RNN), Çok Katmanlı Algılayıcı (MLP) ve Transformer olmak üzere dört model üzerinde durulmuştur. Sonuçlar, GNN modelinin Alzheimer hastalığı için ilgili kanallarda güvenilir yapay EEG sinyalleri üretebildiğini göstermektedir. Ayrıca, önerilen modeller sırasıyla; %99.98, %99.76, %97.58 ve %97.34 gibi yüksek bir doğrulukla doğru sınıflandırma elde etmektedir. Çalışmamız, önerilen metodolojilerin, Alzheimer hastalığının klinik teşhisine yardımcı olabilecek potansiyel biyobelirteçleri belirlemek için umut verici bir tamamlayıcı araç olarak hizmet ettiğini göstermiştir.

Anahtar Kelimeler: Alzheimer Hastalığı (AD), Elektroensefalografi (EEG), Üretken Çekişmeli Ağlar (GNN), Devirli Sinirsel Ağı (RNN), Çok Katmanlı Algılayıcı (MLP) ve Transformer.

FOREWORD

The journey of preparing this thesis on Alzheimer's disease and its early diagnosis has been an enlightening and challenging experience. In this foreword, I aim to provide a brief overview of the purpose, significance, and scope of this study, as well as express my gratitude to those who have supported and contributed to its realization.

Alzheimer's disease is a progressive and irreversible brain disorder that profoundly impacts memory, thinking, and behavior, ultimately leading to dementia. Early diagnosis plays a crucial role in slowing down the disease progression, improving patient care, and enhancing prognosis. Electroencephalography (EEG) has emerged as a promising method for early detection, offering advantages such as affordability, non-invasiveness, and portability. Furthermore, the integration of artificial intelligence tools has proven invaluable in developing models that facilitate disease diagnosis and detection. Deep learning, in particular, holds immense potential for enhancing accuracy; however, it heavily relies on a reliable dataset.

The thesis begins by presenting a Generative Adversarial Networks (GAN) model, which generates artificial EEG datasets for Alzheimer's disease. This model aims to overcome the challenges of accessing a reliable dataset due to patient privacy concerns. The generated dataset serves as a valuable resource for understanding brain processes and enhancing medical diagnoses using deep learning techniques. Additionally, the study focuses on four classification models, namely Convolutional Neural Network (CNN), Recurrent Neural Network (RNN), Multi-layer Perceptron (MLP), and Transformer, to classify Alzheimer's EEG signals. The findings reveal that the GNN model successfully generates reliable artificial EEG signals, showcasing its potential in related channels. These methodologies serve as a promising complementary tool for identifying potential biomarkers, thus aiding in the clinical diagnosis of Alzheimer's disease.

I would like to extend my deepest gratitude to my supervisor, Dr. Öğr. Üyesi Ebubekir KOÇ, whose invaluable mentorship, constructive criticism, experienced guidance, and countless hours of discussions have been instrumental in shaping this work. I am also indebted to Dr. Ahmet Yıldrım from the EEG department at Kartal Dr.

Lütfi Kirdar hospital for his guidance in the diagnosis of EEG signals, which significantly enriched the study. Also, I am profoundly grateful to Turkiye Scholarships (YTB) for granting me the opportunity to pursue my studies in the beautiful country of Turkiye and study at Fatih Sultan Mehmet Vakif university.

In conclusion, this thesis represents a significant contribution to the field of Alzheimer's disease diagnosis and offers a novel approach through the integration of deep learning and artificial intelligence techniques. It is my sincere hope that the findings presented herein will serve as a valuable resource for researchers, clinicians, and practitioners alike in the ongoing battle against Alzheimer's disease.

Husam Al-hammadi

TABLE OF CONTENTS

LIST OF SYMBOLS

$A\beta$	Amyloid
δ	Delta
θ	Theta
α	Alpha
β	Beta
T5	Left Temporal
O1	Left Occipital
P3	Left Parietal
T6	Right Temporal
O2	Right Occipital
P4	Right Parietal
G	Generator
D	Discriminator
pz(z)	Prior Noise Variables
pg	Generator's Distribution
x	Data
Θg	Differentiable Function
x_t	Input
h_t	Hidden State
t	Time
f	Activation Function
o_t	Output
f_t	Forget Gate
i_t	Input Gate
$\tilde{c}_t$	Candidate Memory Cell
c_t	Long-Term Memory Cell
W_{xf}, W_{xi}, W_{xc}, and W_{xg}	Weight Matrices for Input Vector

W_{hf}, W_{hi}, W_{hc}, and W_{hg}	Weight Matrices for The Short-Term State
b_f, b_i, b_c, and b_g	Bias
$\otimes$	Point-Wise Multiplication
$(x1, \ldots, xn)$	Input Sequence
$z = (z1, \ldots, zn)$	Continuous Sequence
$(y1, \ldots, ym)$	Output Sequence
1D	One-Dimensional
P	Power Spectral Density
fs	Sampling Frequency
$\tilde{x}$	Signal Reconstruction
K	Number of Folds
ATotal	Total Number of Accuracies
TP	True Positives
TN	True Negatives
FP	False Positives
FN	False Negatives

LIST OF FIGURES

LIST OF TABLES

LIST OF ABBREVIATION

AD	Alzheimer's Disease
EEG	Electroencephalography
GNN	Generative Adversarial Network
CNN	Convolutional Neural Network
RNN	Recurrent Neural Network
MLP	Multi-Layer Perceptron
BCI	Brain Computer İnterface
CAD	Computer-Aided Diagnosis
MCI	Mild Cognitive Impairment
SMC	Subject Memory Concern
EMCI	Early Mild Cognitive İmpairment
LMCI	Late Mild Cognitive İmpairment
CSF	Cerebrospinal Fluid
MRI	Magnetic Resonance Imaging
PET	Positron Emission Tomography
FDG-PET	Fluorodeoxyglucose Positron Emission Tomography
BOLD	Blood Oxygenation Level-Dependent
fMRI	Functional Magnetic Resonance İmaging
ReLU	Rectified Linear Unit
LSTM	Long Short-Term Memory
ANN	Artificial Neural Network
NLP	Natural Language Processing
Conv-AE	Convolutional Autoencoder
NNs	Neural Networks
TFR	Time-Frequency Representation
PCA	Principal Component Analysis
RPCA	Robust Principal Component Analysis
AAR	Automated Artifact Removal Algorithm
LDA	Linear Discriminant Analysis
QDA	Quadratic Discriminant Analysis

SVM	Support Vector Machine
NB	Naïve Bayes
KNN	K-Nearest Neighbor
DT	Decision Tree
ELM	Extreme Learning Machine
RF	Random Forests
TUH	Temple University Hospital
IRB	Institutional Review Board
EMG	Electromyographic
SEN	Spectral Entropy
REC	Reconstruction Error
R	Real Dataset
AR	Artificial Dataset
RAD	Real Alzheimer Dataset
RH	Real Healthy Dataset
AAD	Artificial Alzheimer's Dataset
MNE	Minimum-Norm Estimation
AUG	Augmented Data
VGG16	Visual Geometry Group
NPY	Numerical Format
MCC	Matthews Correlation Coefficient
SEN	Sensitivity
SPC	Specificity
PPV	Positive Predictive Value

INTRODUCTION

Overview

Dementia is a term used to describe a decline in cognitive function, including memory loss, language difficulties, disorientation, mood swings, and loss of motivation. It is typically caused by physical changes in the brain, such as the accumulation of abnormal protein deposits, damage to nerve cells, or decreased blood flow. Dementia is not itself a single disease but rather a clinical syndrome – that is, a collection of symptoms and other features that exist together and form a recognized pattern. The syndrome of dementia has several causes, although some are more common than others. The common forms of dementia are Alzheimer's disease (AD), Vascular dementia, Frontotemporal dementia, Huntington's disease, and Creutzfeldt-Jacob disease. Alzheimer's disease (AD) is the most common form of advanced dementia observed clinically and it is the source of two-thirds of dementia cases.

Problem Statement

There is currently no proven treatment method for patients who enter the AD stages. Early diagnosis is therefore very important to improve the quality of care and prevent patients from developing further complications. So, diagnosing Alzheimer's disease is one of the most challenging tasks in modern medicine, not just in the early stages of the disease when symptoms are less obvious but also in the later stages of dementia. A variety of approaches and techniques, including Electroencephalography (EEG), biochemical markers, and imaging biomarkers, have greatly aided in the diagnosis of the disease. EEG is considered the most used method, which is a non-invasive technique that measures the electrical activity of the brain. The ability of EEG to detect aberrant brain activity patterns associated with AD has led to its use as a potential diagnostic tool. By analyzing EEG signals and identifying abnormal patterns, clinicians can obtain valuable insights into the progression of the disease and make informed decisions regarding treatment and management. However, neurologists and medical experts still make the majority of manual diagnoses for neurological brain

disorders presently. In some cases, they need several hours to make a final diagnosis for a single patient.

In recent years, researchers in the multidisciplinary fields of bioengineering and neuroscience have made considerable efforts for enhancing the performance of Brain Computer Interface (BCI) and developing a Computer-Aided Diagnosis (CAD) system. The application of deep learning techniques to the classification of Alzheimer's disease based on Electroencephalography (EEG) has gained significant attention due to the recent advancements in artificial intelligence. However, the common point in these methods is that they require large datasets to learn and give accurate results while obtaining EEG data from Alzheimer's patients is problematic. Due to the patient's rights, researchers may not be able to access a sufficient dataset to train the network. As a result, researchers have recently attempted to develop methods and techniques to generate artificial EEG datasets or design signals akin to EEG signals.

Objectives

In this study, the main objective is to create an accessible artificial EEG Alzheimer dataset and classification system by using deep learning methods. Generative Adversarial Network (GNN) will be used for generating EEG Alzheimer dataset and four deep learning models, Convolutional neural Network (CNN), Recurrent Neural Network (RNN), Multi-Layer Perceptron (MLP) and Transformer, will be used for designing classification system. In deep learning, generative modeling is an unsupervised learning task that includes automatically detecting and learning regularities or patterns in input data so that the model may be used to produce or output real examples that could have been drawn from the original dataset. Thus, a group of Alzheimer patients will be examined for EEG signals. The collected data will be filtered and made suitable for the generation process. Following the signal generating procedure, the model's efficiency will be tested using the EEG classification of Alzheimer models, which is based on a classification system.

Research Organization

In addition to this chapter, this research is organized as follows:

Chapter 1 provides medical background and engineering information about Alzheimer's disease and provides deep learning methods discusses which models will be used.

Chapter 2 explains the dataset generation system, as it presents GAN model and shows the process of generating artificial Alzheimer EEG dataset.

Chapter 3 explains the classification system, as it presents deep learning models, describes the structure, and shows classification process.

Chapter 4 discusses the results and shows the conclusion of the research.

CHAPTER 1:

1. BACKGROUND AND LITERATURE REVIEW

1.1. ALZHEIMER'S DISEASE

1.1.1. Definition

Dementia is a condition characterized by cognitive impairment that is severe enough to cause a decline in mental, behavioral, and social abilities. Clinically, Alzheimer's disease (AD) is the most frequently diagnosed type of progressive dementia and accounts for approximately two-thirds of all dementia cases (Dening & Sandilyan, 2015). Alzheimer's disease (AD) is a neurodegenerative disease that results in brain atrophy and cell death (Dubois et al., 2016; Scheltens et al., 2016).

The disease was diagnosed in 1907 by Alois Alzheimer, a German psychiatrist and neuropathologist (Alzheimer, 1907). Although the pathogenesis of the disease is still unknown, it is assumed that an abnormal build-up of proteins in and around brain cells may cause the disease (Jonker, Launer, Hooijer, & Lindeboom, 1996). One of the proteins involved in amyloid (Aβ) deposits causes plaques around the brain cells; consequently, the neural bonds between brain cells are severed (Mattson, 2004; Scheltens et al., 2016).

AD is the third most costly disease in the United States and the sixth leading cause of death. It affects more than 10% of Americans over the age of 65 and nearly half of those over the age of 85. However, the number of people living with Alzheimer's disease in the United States is rising. An estimated 6.5 million Americans aged 65 and older will live with Alzheimer's in 2022 (Alzheimer's & dementia, 2022). By 2050, Alzheimer's dementia is expected to affect 12.7 million people in the United States (Alzheimer's & dementia, 2022). The impact of AD extends beyond the individual affected and can have significant social and economic consequences. As the number of people affected by AD continues to grow, it is essential to identify effective diagnostic and treatment strategies to manage the disease and its associated.

1.1.2. Stages of Alzheimer's Disease

According to the National Institute on Aging ("Alzheimer's Disease Fact Sheet," July 08, 2021) and the Alzheimer's Association ("Stages of Alzheimer's,"), the progression of the disease can be classified into three different stages. The first stage is Mild Cognitive Impairment (MCI), which can be mainly divided into subject memory concern (SMC), early mild cognitive impairment (EMCI), and late mild cognitive impairment (LMCI). At this stage the patient's cognition begins to gradually deteriorate, which causes a wide range of symptoms, such as including difficulties remembering recent events, subtle behavioural changes, distinct loss of autonomy in daily activities, confusion about time and place, and personality changes. The second stage is Moderate Alzheimer's disease. This stage of the disease involves significant memory loss, difficulty with language and communication, and problems with mobility and coordination. Patients may also experience changes in behavior, such as wandering, agitation, or aggression in this stage. The last stage is Severe Alzheimer's disease, in which brain tissue significantly shrinks as plaques and tangles spread throughout the brain. At the stage of disease progress, continuous and strict supervision is required due to the patients being unable to perform any tasks ("Alzheimer's Disease Fact Sheet," July 08, 2021; Rodrigues, Teixeira, Garrett, Alves, & Freitas, 2016; "Stages of Alzheimer's,").

1.1.3. Alzheimer's Disease Diagnosis

Since AD is an incurable disease, early diagnosis is one of the primary methods to increase the quality and quantity of patient care. Thus, diagnosing the disease is one of the most challenging tasks in modern medicine, not just in the early stages of the disease when symptoms are less obvious but also in the later stages of AD. Several methods, such as biochemical markers, imaging biomarkers, and Electroencephalography, have contributed to and significantly assisted in diagnosing the disease.

In biochemical markers, biochemical tests are used for measuring the protein concentrations of beta-amyloid, total tau protein and phosphorylate tau181P the cerebrospinal fluid (CSF) or blood (Rabbito, Dulewicz, Kulczyńska-Przybik, & Mroczko, 2020; Sunderland et al., 2006). These tests can help to diagnose Alzheimer's

disease and monitor disease progression. Furthermore, imaging biomarkers, such as Magnetic Resonance Imaging (MRI) and Positron Emission Tomography (PET), have played a significant role in understanding the diagnosis process. In PET, several types of scans are used to determine the concentration of particular molecules in the brain. E.g., Fluorodeoxyglucose Positron Emission Tomography (FDG-PET) is a test used to the uptake of a radioactive glucose tracer in the brain, which provides information about brain metabolism and function (Johnson, Fox, Sperling, & Klunk, 2012; Marcus, Mena, & Subramaniam, 2014; Weiner & aging, 2009).

Since Alzheimer's disease is characterized by an insidious onset and inexorable progression of atrophy in the brain, MRI can show changes in brain structure, including shrinkage of the hippocampus, a region of the brain important for memory formation and retrieval (Scheltens, Fox, Barkhof, & De Carli, 2002). Also, another imaging technique is known as Resting-state fMRI, which is a technique that measures spontaneous fluctuations in blood oxygenation level-dependent (BOLD) signal in the brain. BOLD fMRI is a method used to measure the changes in blood oxygen levels in neurons and this method has been used to investigate changes in functional connectivity patterns in the brain for AD patients (Ogawa, Lee, Nayak, & Glynn, 1990). This technique is considered more functional for monitoring disease progression in later stages (van Oostveen & de Lange, 2021).

1.2. ELECTROENCEPHALOGRAPHY

Electroencephalography (EEG) is a method used to measure the electromagnetic field activity of brain cells. EEG signals are typically separated into several frequency bands, including delta (δ, 0.5-4 Hz), theta (θ, 4-8 Hz), alpha (α, 8-13Hz), and beta (β, 13-30 Hz) as shown in figure 1.1 (Stern, 2005). Each frequency band is associated with different physiological and cognitive processes, and their analysis can provide valuable insights into the underlying neural activity. Delta waves, for instance, are typically observed in EEG signals of sleeping individuals, while alpha waves are commonly observed when the individual is awake but relaxed and not paying attention to external stimuli. Theta waves are frequently observed in states of deep relaxation, while beta waves are typically detected in EEG signals when an

individual is actively engaged in mental activity or sensory processing (Sanei & Chambers, 2013).

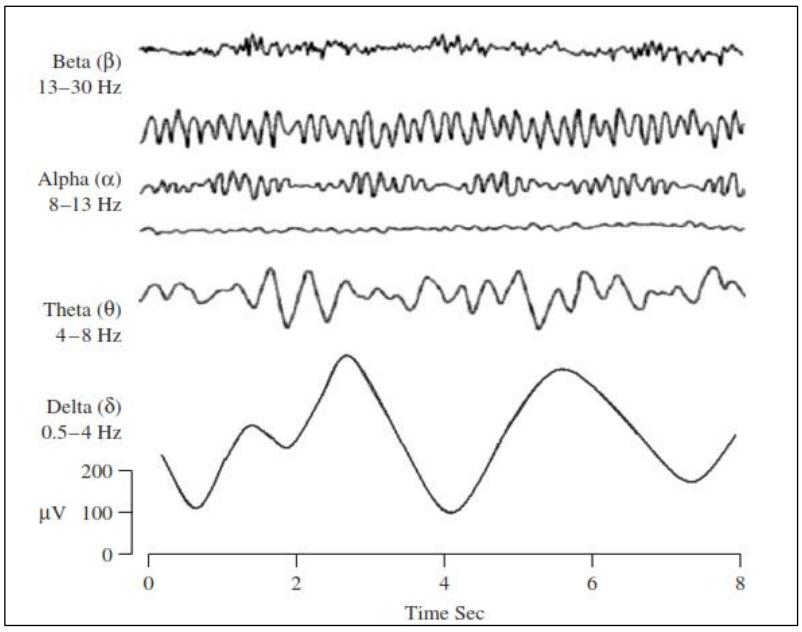

Figure 1. 1 The normal brain frequency with their amplitude levels (Sanei & Chambers, 2013).

Research has shown that Alzheimer's disease (AD) affects the power of electrical signals in different frequency bands in the brain. The most commonly observed effect is referred to as "EEG slowing" (Sanei & Chambers, 2013), which is characterized by an increase in power in the low-frequency bands, such as delta and theta, and a reduction in power in the higher frequency bands, such as alpha and beta (Jeong, 2004; Malek, Baker, Mann, & Greene, 2017).

EEG has been recognized as an effective method for recording abnormal brain activity patterns, particularly in AD, due to its noninvasive and inexpensive nature, high resolution, and direct access to neuronal signals. Unlike functional magnetic resonance imaging (fMRI) or positron emission tomography (PET), which detect metabolic signals indirectly, EEG provides a direct measurement of neuronal activity, making it a valuable tool for understanding the pathophysiology of AD. The ability of EEG to detect aberrant brain activity patterns associated with AD has led to its use as a potential diagnostic tool. By analyzing EEG signals and identifying abnormal patterns, clinicians can obtain valuable insights into the progression of the disease and make informed decisions regarding treatment and management.

In Alzheimer's disease, the brain undergoes significant changes, including the degeneration of neurons and the formation of amyloid plaques and neurofibrillary tangles. These changes can affect the synchronization of electrical activity in the brain, which can be measured using EEG synchronization channels. EEG synchronization channels have been used to study the effects of Alzheimer's disease on the brain, and research has shown that in patients with Alzheimer's disease, there is a reduction in alpha and beta band synchronization in the occipital and temporal regions of the brain (Al-Jumeily, Iram, Vialatte, Fergus, & Hussain, 2015; Rice et al., 1990). These regions are involved in visual processing and memory, respectively, which are often affected by Alzheimer's disease. The study focused on four channels (Left Temporal-Left Occipital (T_5-O_1), Left Parietal-Left Occipital (P_3-O_1), Right Temporal-Right Occipital (T_6-O_2), Right Parietal-Right Occipital (P_4-O_2) as can be seen in Figure 1.2.

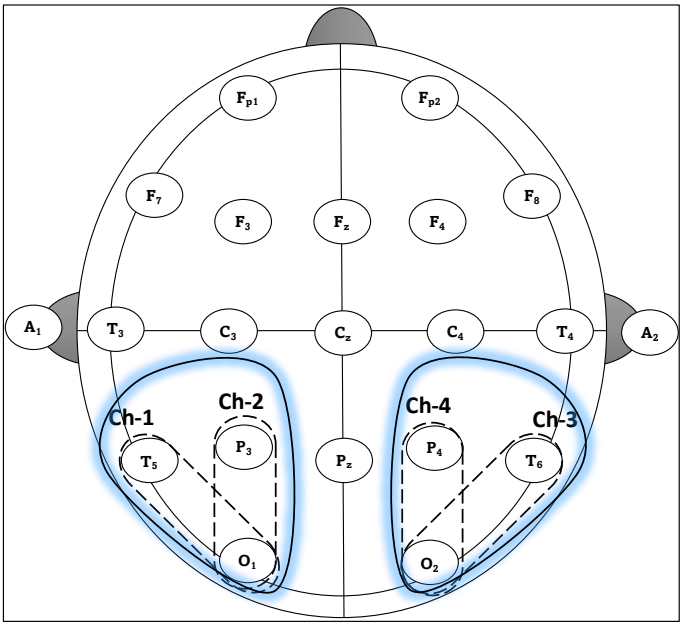

Figure 1. 2 The 4-channels used for generating and classifying Alzheimer's EEG signals.

1.3. DEEP LEARNING MODELS

In recent years, researchers in the multidisciplinary fields of bioengineering and neuroscience have made considerable efforts for enhancing the performance of Brain Computer Interface (BCI) and developing a Computer-Aided Diagnosis (CAD) system. The application of deep learning techniques to the classification of Alzheimer's disease based on electroencephalography (EEG) has gained significant

attention due to the recent advancements in artificial intelligence. Deep learning models, including Convolutional Neural Network (CNN), Recurrent Neural Network (RNN), Multi-Layer Perceptron (MLP), and Transformer, have been extensively explored for their potential in accurately classifying EEG signals associated with Alzheimer's disease. There are also many models used, however, the models that have been used in this work will be explained in this section.

1.3.1. Generative Adversarial Network

Generative Adversarial Network (GAN) is an unsupervised learning technique that has shown promising results for learning complex distributions. It consists of two neural networks, a generator (*G*) and a discriminator (*D*). The generator network takes random noise as input and generates a sample that mimics the true data distribution. The discriminator network takes a sample and classifies it as real (from the true data distribution) or fake (generated by the generator). The model was proposed in 2014, summarized in Equation 1 (Goodfellow et al., 2014).

$$min_G max_D V(D,G) = E_{x\sim P_{data(x)}}[\log D(x)] + E_{z\sim P_{z(z)}}\left[\log\left(1 - D\left(G(z)\right)\right)\right] \quad (1)$$

This equation briefly explains adversarial modelling as both (*G*, *D*) have multilayer models. Prior noise variables *pz(z)* have been established as input to learning the generator's distribution *pg* over data *x*. Then a mapping to data space is represented as *G (z; Θg),* where *G* is a differentiable function represented by a convolutional neural network with parameters *Θg*. Second convolutional neural networks have been defined as *D (x; Θd)*, which outputs a single scalar. The probability that *x* came from the data rather than *pg* is represented as *D(x)*. The purpose of the equation is to train *D* to maximize the probability of assigning the correct label to both training examples and samples from *G*. It is trained to minimize *log(1-D(G(z)))*, in which *D* and *G* play the following two-player minimax game with value function *V (G; D)*, as can be seen in the Equation 1 (Goodfellow et al., 2014). A block diagram illustrating the GANs model is shown in Figure 1.3.

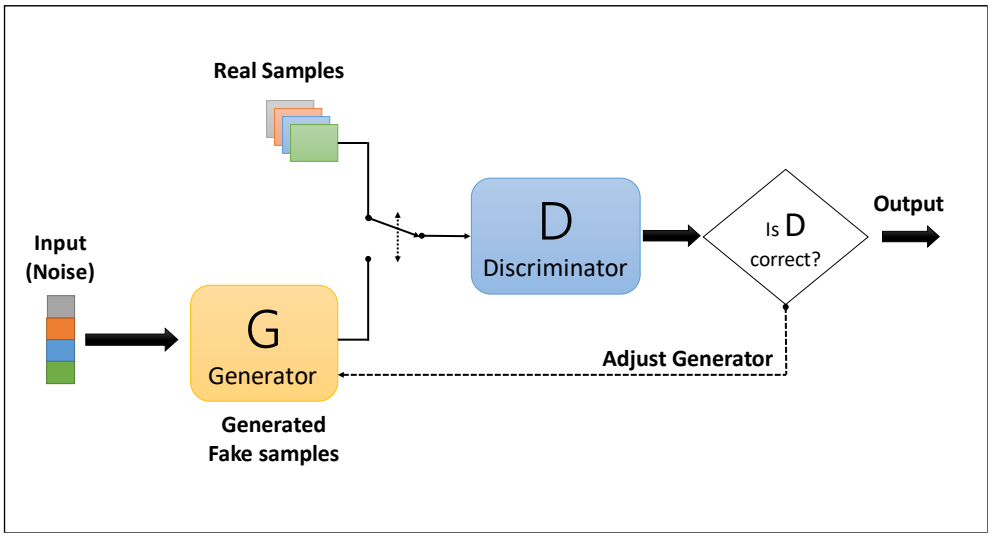

Figure 1. 3 Block diagram of the GAN model.

1.3.2. Convolutional neural Network

Convolutional Neural Network (CNN) is a powerful deep learning algorithm that is widely used for image and video analysis. One of the key features of CNN is their ability to extract relevant features from input data, such as edges, corners, or other patterns, by using a series of convolutional layers with learnable filters that slide over the input data (Ajit, Acharya, & Samanta, 2020; O'Shea & Nash, 2015). The output from each convolutional layer is then passed through a nonlinear activation function, such as the rectified linear unit (ReLU), to introduce nonlinearity to the model. The output from the final convolutional layer is then fed into one or more fully connected layers, which perform a classification or regression task (Li et al., 2021).

A typical CNN architecture consists of three types of layers, namely convolutional layers, pooling layers, and fully connected layers, which are stacked together to form a deep neural network. In the convolutional layers, the filters slide over the input data to extract useful features, while the pooling layers downsample the feature maps to reduce their size and extract more robust features. Finally, the fully connected layers use the extracted features to perform a classification or regression task (O'Shea & Nash, 2015). To illustrate a simplified CNN architecture for MNIST classification, Figure 1.4 is provided.

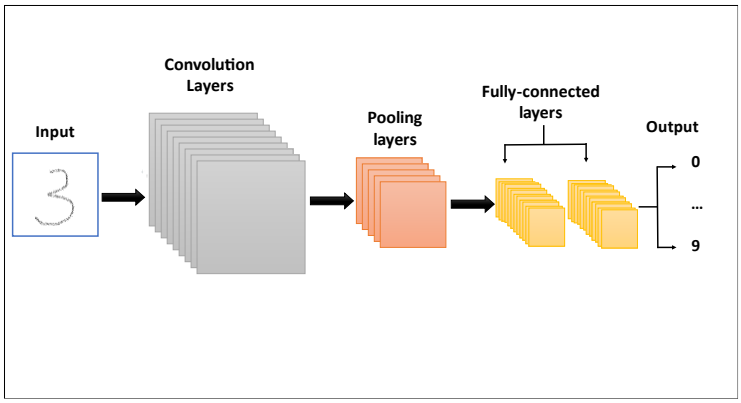

Figure 1. 4 A simple CNN architecture.

1.3.3. Recurrent Neural Network

Recurrent Neural Network (RNN) is a type of artificial neural network that is designed to handle sequential data, such as time-series data or sequential text data. Recurrent Neural Network (RNN) differs from standard neural networks in their ability to process sequential data by maintaining an internal state or memory of previous inputs (Yu, Si, Hu, & Zhang, 2019). Unlike standard neural networks, which process input data as a fixed-size vector or tensor, RNN process sequences of variable length, such as sentences, audio signals, or time-series data. This is achieved by introducing connections between neurons that allow information to flow backwards from the current output to the previous inputs, effectively creating a loop that enables the network to maintain a memory of previous inputs (Medsker, Jain, & Applications, 2001). Figure 1.5 provides a simple RNN architecture.

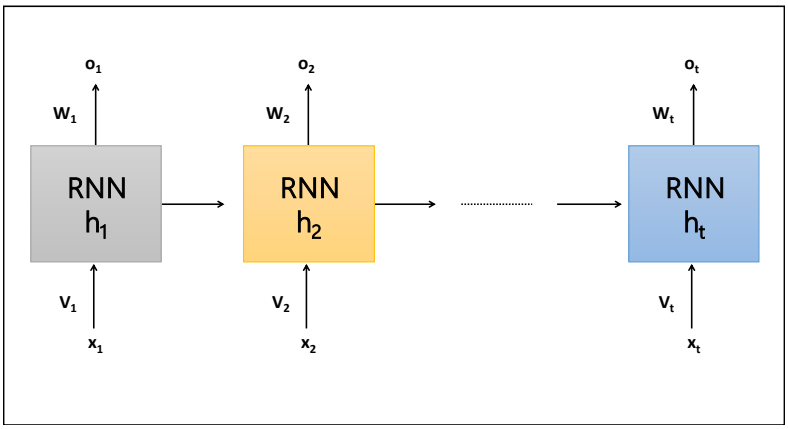

Figure 1. 5 A simple RNN architecture.

In this architecture, the RNN processes input sequences by taking an input x_t and a hidden state h_{t-1} at each time step t. The hidden state h_{t-1} is passed from the previous time step, allowing the network to maintain a memory of previous inputs. This is achieved by introducing connections between neurons that allow information to flow backwards from the current output to the previous inputs, effectively creating a loop that enables the network to maintain a memory of previous inputs. The equations (2) and (3) represent the mathematical operations performed at each time step of the RNN (Alessandrini et al., 2022; Yu et al., 2019).

$$h_t = f(W_h h_{t-1} + V_h x_t + b_h) \quad (2)$$

$$o_t = f(W_o h_t + b_o) \quad (3)$$

Equation (2) represents the computation of the new hidden state h_t by taking the previous hidden state h_{t-1}, the current input x_t, and the weights and biases of the hidden layer as inputs. The activation function f applies a non-linear transformation to the linear combination of these inputs. This allows the network to learn complex patterns in sequential data and capture long-term dependencies. Equation (3) represents the computation of the output o_t by taking the new hidden state h_t and the weights and biases of the output layer as inputs. The activation function f applies a non-linear transformation to the linear combination of these inputs, resulting in the output of the network at that time step (Alessandrini et al., 2022).

One of the key challenges in training RNN is the problem of vanishing gradients, which occurs when the gradient of the loss function with respect to the weights becomes very small as it is propagated backwards through time. This can make it difficult for the network to learn long-term dependencies (S. J. I. J. o. U. Hochreiter, Fuzziness & Systems, 1998). To address this issue, various modifications to the basic RNN architecture have been proposed, such as Long Short-Term Memory (LSTM) networks by Hochreiter et al. (S. Hochreiter & Schmidhuber, 1997), which use additional gating mechanisms to control the flow

of information through the network and allow it to selectively remember or forget certain inputs. The structure of the LSTM unit is shown in Figure 1.6.

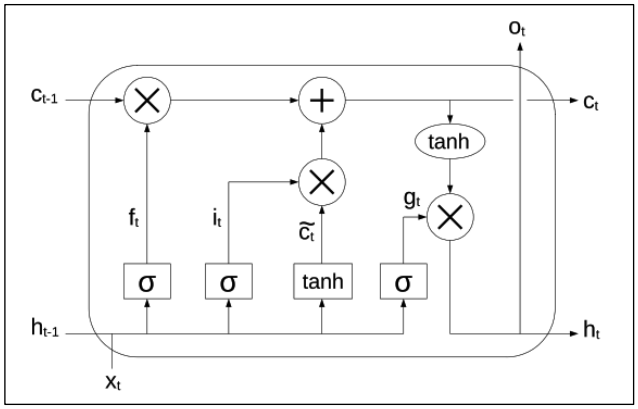

Figure 1. 6 The structure of the LSTM unit (Alessandrini et al., 2022).

The Long Short-Term Memory (LSTM) architecture is a modification to the basic RNN architecture that uses additional gating mechanisms to selectively control the flow of information through the network, thereby enabling it to overcome the problem of vanishing gradients and learn long-term dependencies (S. J. I. J. o. U. Hochreiter, Fuzziness & Systems, 1998). In LSTM networks, the long-term state, short-term state, and the output of each layer at each time step are described by a set of equations. The forget gate f_t determines how much of the previous long-term state to forget, while the input gate it determines how much of the new input to add to the current long-term state (S. Hochreiter & Schmidhuber, 1997). The output gate o_t is used to control the output of the current time step. The equations that define the behavior of an LSTM unit are as follows (Alessandrini et al., 2022):

$$f_t = \sigma\left(W_{x_f}^T x_t + W_{h_f}^T h_{t-1} + b_f\right) \quad (4)$$

$$i_t = \sigma\left(W_{x_i}^T x_t + W_{h_i}^T h_{t-1} + b_i\right) \quad (5)$$

$$\tilde{c}_t = tanh\left(W_{x_c}^T x_t + W_{h_c}^T h_{t-1} + b_c\right) \quad (6)$$

$$g_t = \sigma\left(W_{x_g}^T x_t + W_{h_g}^T h_{t-1} + b_g\right) \quad (7)$$

$$c_t = f_t \otimes c_{t-1} + i_t \otimes \tilde{c}_t \quad (8)$$

$$o_t = h_t = g_t \otimes \tanh(c_t) \quad (9)$$

The forget gate f_t is determined by the sigmoid activation function and is defined by the equation (4). The input gate i_t is also determined by the sigmoid function and is defined by the equation (5). The candidate memory cell $\tilde{c}_t$ is calculated using the hyperbolic tangent function and is defined by the equation (6). The output gate o_t is calculated using the sigmoid function and is defined by the equation (7). The long-term memory cell c_t is updated using a combination of the forget gate ft and the input gate i_t, as well as the candidate memory cell $\tilde{c}_t$. This is defined by the equation (8). Finally, the short-term memory state h_t and the output o_t are calculated using the output gate o_t and the hyperbolic tangent of the updated long-term memory cell c_t, as defined by the equations (9). In these equations, W_{xf}, W_{xi}, W_{xc}, and W_{xg} represent the weight matrices associated with the matching connected input vector, while W_{hf}, W_{hi}, W_{hc}, and W_{hg} are the weight matrices for the short-term state from the previous time step. The bias terms b_f, b_i, b_c, and b_g are added to each gate and memory cell. The symbol $\otimes$ denotes the point-wise multiplication (Alessandrini et al., 2022).

1.3.4. Multi-Layer Perceptron

The Multi-Layer Perceptron (MLP) is a powerful type of Artificial Neural Network (ANN) that is widely used for a variety of tasks, including classification, regression, and prediction. It consists of multiple layers of interconnected neurons, with each neuron in a layer fully connected to all neurons in the previous and next layers. This allows the MLP to learn complex non-linear relationships between input and output data. In an MLP, the input is passed through one or more hidden layers of neurons, each layer performing a linear transformation of the input followed by a non-linear activation function, such as the sigmoid or ReLU function. The activation function introduces non-linearity into the network, enabling it to learn more complex and sophisticated patterns in the data. The final output of the MLP is typically produced by a single output layer of neurons, which performs a linear transformation of the output of the last hidden layer followed by a non-linear

activation function. The output layer is often designed to produce a probability distribution over the possible output classes or values. The general structure of an MLP is shown in Figure 1.7, with input layer, one or more hidden layers, and output layer. The size and number of hidden layers and the number of neurons in each layer can be customized to suit the specific task at hand (Kruse, Mostaghim, Borgelt, Braune, & Steinbrecher, 2022).

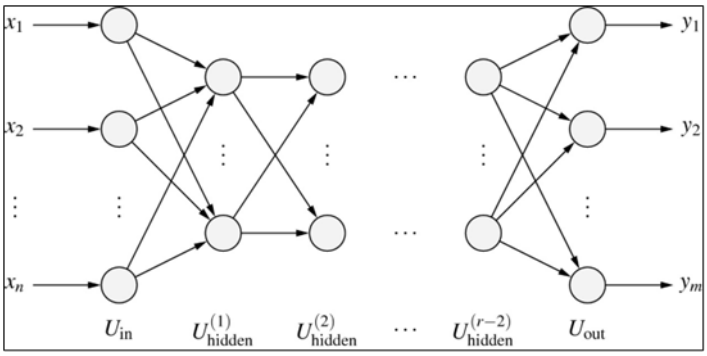

Figure 1. 7 The structure of the MLP unit (Kruse et al., 2022).

The network input function of each hidden and output neuron can be expressed as the weighted sum of the inputs, where the weights are the connection weights between the input and the neuron. In mathematical terms, for all u belonging to the set of hidden neurons union set of output neurons (Kruse et al., 2022), the network input function can be defined as:

$$\forall_u \in U_{hidden} \cup U_{out} : \quad f_{net}^{(u)}(in_u, w_u) = w_u\, in_u = \sum_{v \in pred(u)} w_{uv}\, out_v \qquad (10)$$

Where, in_u is the input to the neuron, w_u is the weight of the connection between the input and the neuron, and out_v is the output of the neuron v that connects to the neuron u. The symbol Σ represents the sum over all the neurons v that are predecessors of the neuron u.

1.3.5. Transformer

The Transformer is a deep learning model that was introduced in 2017 by Vaswani et al. (Vaswani et al., 2017) for Natural Language Processing (NLP) tasks

such as language translation, language modeling, and text generation. It is based on the self-attention mechanism, which allows the model to weigh the importance of different parts of the input sequence when generating the output. Unlike traditional recurrent neural network (RNN) models that process input sequences in a sequential manner, the Transformer model processes the entire input sequence in parallel, which allows it to capture long-range dependencies more efficiently. It consists of an encoder and a decoder, each of which contains multiple layers of self-attention and feedforward neural networks. The encoder takes the input sequence and produces a sequence of hidden representations, each of which captures information from the entire input sequence. The decoder takes the encoder output and generates the output sequence one token at a time, using the self-attention mechanism to attend to different parts of the input sequence as needed (Tay, Dehghani, Bahri, & Metzler, 2022). The Transformer follows this overall architecture using stacked self-attention and point-wise, fully connected layers for both the encoder and decoder, shown in the left and right halves of Figure 1.8, respectively (Vaswani et al., 2017).

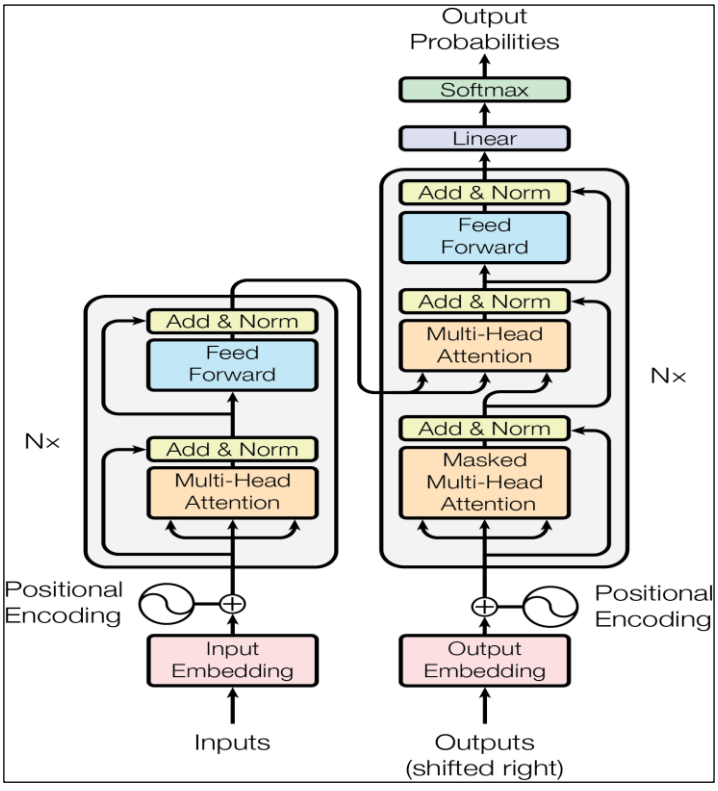

Figure 1. 8 The structure of the Transformer respectively (Vaswani et al., 2017).

The Transformer model consists of an encoder and a decoder, both of which are composed of multiple layers. The encoder takes an input sequence of symbol representations *(x1, …., xn)* and maps it to a sequence of continuous representations *z = (z1, …., zn).* Each layer in the encoder consists of two sub layers: a multi-head self-attention mechanism and a position-wise fully connected feedforward network. The self-attention mechanism allows the model to weigh the importance of different positions in the input sequence when computing the output at each position, while the feedforward network applies a non-linear transformation to each position separately and identically. The decoder, on the other hand, takes the continuous representations *z* and generates an output sequence *(y1, …., ym)* of symbols one element at a time. Like the encoder, each layer in the decoder consists of two sub-layers: a multi-head self-attention mechanism and a position-wise fully connected feedforward network. In addition, the decoder also includes a third sub-layer, which applies a multi-head attention mechanism to the encoder output *z* and computes a context vector for each position in the decoder input (Vaswani et al., 2017).

1.4. RELATED WORKS

The application of deep learning techniques to the classification of Alzheimer's disease based on Electroencephalography (EEG) has gained significant attention due to the recent advancements in artificial intelligence. Deep learning models, including Convolutional Neural Network (CNN), Recurrent Neural Network (RNN), Multi-Layer Perceptron (MLP), and Transformer, have been extensively explored for their potential in accurately classifying EEG signals associated with Alzheimer's disease. For instance, previous studies have demonstrated the effectiveness of CNN in identifying and classifying Alzheimer's signals (Fouladi, Safaei, Mammone, Ghaderi, & Ebadi, 2022; C. Ieracitano, N. Mammone, A. Hussain, & F. C. Morabito, 2020a; Morabito et al., 2016). *Morabito et al.* (Morabito et al., 2016) utilized CNN to extract relevant features from EEG signals, which were then used as inputs to a classifier, achieving an accuracy of 82% in classifying EEG signals of AD patients and healthy controls (Morabito et al., 2016). *Ieracitano et al.* (Ieracitano et al., 2020a) proposed a novel approach by developing a customized CNN that can self-learn relevant features directly from the analysis of EEG recordings without the need for any hand-crafted

feature extraction technique. Their approach achieved an accuracy of 85% in classifying EEG signals of AD patients and healthy control (Ieracitano et al., 2020a). *Fouladi et al.* (Fouladi et al., 2022) also modified CNN and Convolutional Autoencoder (Conv-AE) Neural Network (NN) and employed Time-Frequency Representation (TFR) to extract desirable features from EEG signals. The average accuracy obtained in this work is 92% (Fouladi et al., 2022).

Recurrent Neural Network (RNN) is also being used to classify Alzheimer's signals from EEG recordings. RNN has been used in EEG analysis for Alzheimer's disease by learning the patterns in the EEG signals and using this information to classify the signals as indicating Alzheimer's disease or not. *Alessandrini et al.* (Alessandrini et al., 2022) developed RNN model on EEG data that has been pre-processed with traditional Principal Component Analysis (PCA). The RNN is then trained on this processed data. After that, the researchers use corrupted data as input and process it with Robust Principal Component Analysis (RPCA) to filter outlier components. This combined approach allows for the identification of Alzheimer's patterns, and the results of this approach reached to 93.5% (Alessandrini et al., 2022). Another work reported by *Alvi et al.* (Alvi, Siuly, & Wang, 2022) provided a deep learning-based framework using the Long Short-term Memory (LSTM) model for identifying of MCI patients from healthy patients. In their study, they showed that the LSTM was able to achieve a performance of up to 96.41% in classifying EEG signals as indicative of MCI or not (Alvi et al., 2022).

Multi-layer Perceptron (MLP) is a popular type of neural network that has also been used for classifying Alzheimer's EEG signals. In Alzheimer's EEG analysis, MLP has been employed to classify EEG signals as indicative of Alzheimer's disease or not by detecting patterns in the signals. For example, *Ieracitano et al* (C. Ieracitano, N. Mammone, A. Hussain, & F. C. J. N. N. Morabito, 2020b) proposed a multi-modal machine learning-based approach for automatically classifying EEG recordings in dementia, achieving a high accuracy rate of 97% (Ieracitano et al., 2020b). In addition, machine learning techniques have shown great potential in the classification of Alzheimer's disease using EEG signals. For instance, *Cassani et al.* (Cassani et al., 2017) used an automated EEG-based AD diagnostic system based on an Automated Artifact Removal (AAR) algorithm and a low-density (7-channel) EEG setup. The

proposed diagnostic system had a maximum accuracy of 91.4% (Cassani et al., 2017). Another work reported by *Alsharabi et al.* (AlSharabi, Salamah, Abdurraqeeb, Aljalal, & Alturki, 2022) which used machine learning approaches to classify EEG signals. They used Linear Discriminant Analysis (LDA), Quadratic Discriminant Analysis (QDA), Support Vector Machine (SVM), Naïve Bayes (NB), K-Nearest Neighbor (KNN), Decision Tree (DT), Extreme Learning Machine (ELM), Artificial Neural Network (ANN), and Random Forests (RF). The performances of the different proposed machine learning approaches have been evaluated and the best classification accuracy achieved in KNN classifier achieved which is 99.98% (AlSharabi et al., 2022).

Transformer-based models have been used in EEG classification tasks. Transformer-based models have been used to classify EEG signals into different categories, such as different types of sleep stages or different diseases, based on the patterns in the signals (Guo et al., 2022; Sun, Xie, & Zhou, 2021; Wang, Wang, Hu, Yin, & Song, 2022). Transformer-based models have been shown to be effective in EEG analysis and have been used in several studies to achieve high levels of classification accuracy. However, this area of research is still in its early stages and more research is needed to fully understand the potential of Transformer-based models in EEG analysis.

CHAPTER 2:

2. DATASET GENERATION SYSTEM

2.1. DATASET

2.1.1. Alzheimer EEG Dataset

The GAN model must employ a real EEG signals dataset to generate artificial EEG Alzheimer's signals. Thus, we have employed a clinical EEG dataset collected from archival records at Temple University Hospital (TUH) named "TUH Abnormal EEG Corpus" (Obeid & Picone, 2016). The dataset was collected under the Declaration of Helsinki with the permission of the Temple University IRB (Obeid & Picone, 2016).

A set of 44 subjects (20 patients) were selected, as seen in Table 2.1, as their diagnoses and patient histories contained Alzheimer's based on experts at the Temple University Hospital. The evaluation step has been established manually with the help of a specialist from Kartal Dr. Lütfi Kirdar Hospital of Istanbul was engaged to ensure they include Alzheimer's disease.

Table 2. 1 The EEG Alzheimer dataset.

Gender	Age Range	Number of subjects	Number of patients	Duration (minute)
Female	59 - 92	25	13	269.9 m
Male	53 - 93	19	7	278.5 m

2.1.2. Dataset Preprocessing

The dataset needed to go through some preliminary preprocessing before being used as the input for the subsequent phases. First, it was observed that the set of signals included in each subject's data varied slightly, ranging from 21 to 23 channels from a list of possible channels such as Fp1, Fp2, Fpz, EKG, F7, F3, Fz, F4, F8, C3, Cz, C4, T3, T4, T5, T6, P3, Pz, P4, O1, O2, I, II, MK. Additionally, the order of these channels differed across subjects. To ensure a coherent and consistent set of input data, a subset of common signals present in all subjects was isolated. This resulted in a set of 16

signals, namely: Fp1, Fp2, F7, F3, F4, F8, T3, C3, C4, T4, T5, P3, P4, T6, O1, O2. These signals were then extracted and reordered accordingly. Moreover, to facilitate further processing in the subsequent steps, the data were saved in the "*npy*" format, which is a numerical format commonly used in Python's NumPy library. This format offers convenience and efficiency in handling the data.

Furthermore, considering that Alzheimer's disease manifests more prominently in specific channels, the transformed channels were reduced to four channels: [T5-O1], [P3-O1], [T6-O2], and [P4-O2]. These channels were selected based on their relevance to capturing the characteristic patterns associated with Alzheimer's disease.

EEG signals are highly susceptible to noise, which can adversely affect the accuracy of the analysis. To address this issue, preprocessing techniques are employed to remove noise and artifacts from the EEG signals before they are used to train the deep learning model. One widely used software package for preprocessing EEG data is MNE (Gramfort et al., 2014), which provides various functions for filtering, artifact removal, and other preprocessing steps.

MNE has been used to preprocess EEG datasets for Alzheimer's disease analysis, specifically by removing interference and eliminating ocular artifacts and electromyographic signals (EMG). Various preprocessing functions provided by MNE were employed to address these concerns effectively. For instance, functions such as *EOGRegression* were used to remove unwanted signals originating from ocular movements, *annotate_muscle_zscore* was utilized to detect and eliminate muscle-related artifacts, and *annotate_movement* helped in identifying and mitigating movement-related artifacts. Moreover, the EEG signals are manually examined to ensure that they are free from unwanted signals and artifacts. Finally, the processed EEG channels were organized into segments of 10s equal to 2500 samples (1576 epochs). By employing these preprocessing techniques, the EEG datasets were cleansed from unwanted signals, enabling more accurate and reliable analysis for Alzheimer's disease research.

2.2. GAN MODEL

2.2.1. Discriminator Model (D)

The discriminator model is responsible for distinguishing whether the signal is real (Alzheimer's EEG signals) or artificial (induced by a generator). Our model, Visual Geometry Group (VGG16) is employed as a discriminator, a well-known Convolutional Neural Networks (CNNs) model with 16 layers. VGG16 has been widely used in various image processing tasks and has demonstrated excellent performance in 2D convolutional neural networks (Simonyan & Zisserman, 2014).

Since our dataset is one-dimensional (1D), we have to modify the VGG16 model to fit the dataset where every layer is converted to its corresponding in 1D. Our VGG16 model consists of 16 layers, beginning with 13 *Conv1D layers* with filter sizes of 64, 128, 256, and 512, and kernel sizes of 3, 5, and 7. We have also included five *MaxPooling layers* with two filters of stride two between the convolutional layers. The *ReLU* activation function is used for all the convolutional layers to allow gradients to be back-propagated during training and to prevent negative values from being passed to the next layer (Xu, Wang, Chen, & Li, 2015). The last three layers of our VGG16 model are fully connected layers, with two layers of 4096 units using the *ReLU* activation function and an output layer of one unit using the *sigmoid* activation function.

This architecture is designed to learn high-level features from the input signals and make a binary decision on whether the signal is real or artificial. By adapting the VGG16 model to the 1D signal domain, our discriminator can effectively distinguish between real and generated signals and help to improve the overall performance of our GAN model.

2.2.2. Generator Model (G)

The latent space is a vector space of Gaussian-distributed values that is randomly sampled and provided as input to the generator model during training. During training, the generator learns to map points in the latent space to output EEG signals that are similar to real Alzheimer's EEG signals. At the end of training, the generator has learned to assign meaning to points in the latent space, such that specific regions of the space correspond to specific features of the output EEG signals. By

sampling points from the latent space and providing them as input to the generator, new plausible Alzheimer's EEG signals can be generated. *J. Brownlee's* (Brownlee, 2019) proposed model was used and modified to suit our work.

The generator model consists of eight layers, with the first being a *dense layer* with enough nodes to represent a low-resolution version of the output signal. The activations from this layer are then *reshaped* into a signal representation to be fed into a convolutional layer with 128 different 625 feature maps. For the *unsampling* process, we utilized five layers arranged as follows: a *Conv1DTranspose layer* with 128 filters of stride 2, two *Conv1D layers* with 128 filters and a kernel size of (5, 7), another *Conv1DTranspose layer* with 128 filters of stride 2, and a *Conv1D layer* with 128 filters and a kernel size of 5. We selected the leaky rectified linear activation (*LeakyReLU*) with a slope of 0.2 (Xu et al., 2015) as the activation function between these layers. The output layer is a *Conv1D* with one filter and a kernel size of 7, and a *sigmoid* activation function is applied to guarantee that output values are normalized between [0, 1]. The *Adam* optimizer with a learning rate of 0.0002 and a momentum of 0.5 is utilized in both models (D, G).

In this chapter, we have been describing the steps involved in developing a dataset generation system for Alzheimer's EEG datasets. These steps are illustrated in Figure 2.1. In the beginning, the data for the discriminator are defined as real/fake signals, and it is trained to distinguish between them. Then, the generator transforms random noise into artificial Alzheimer's signals and sends them to the discriminator. The purpose of the discriminator is to determine whether the input comes from a generator network or a real dataset. Suppose the artificial Alzheimer's signals are detected by the discriminator. In that case, feedback is sent to the generator for enhancing and adjusting the networks until it generates artificial Alzheimer's signals that cannot be detected by the discriminator. Through this training process, the generator learns to produce signals that can deceive the discriminator, resulting in a high-quality output that closely resembles the real data.

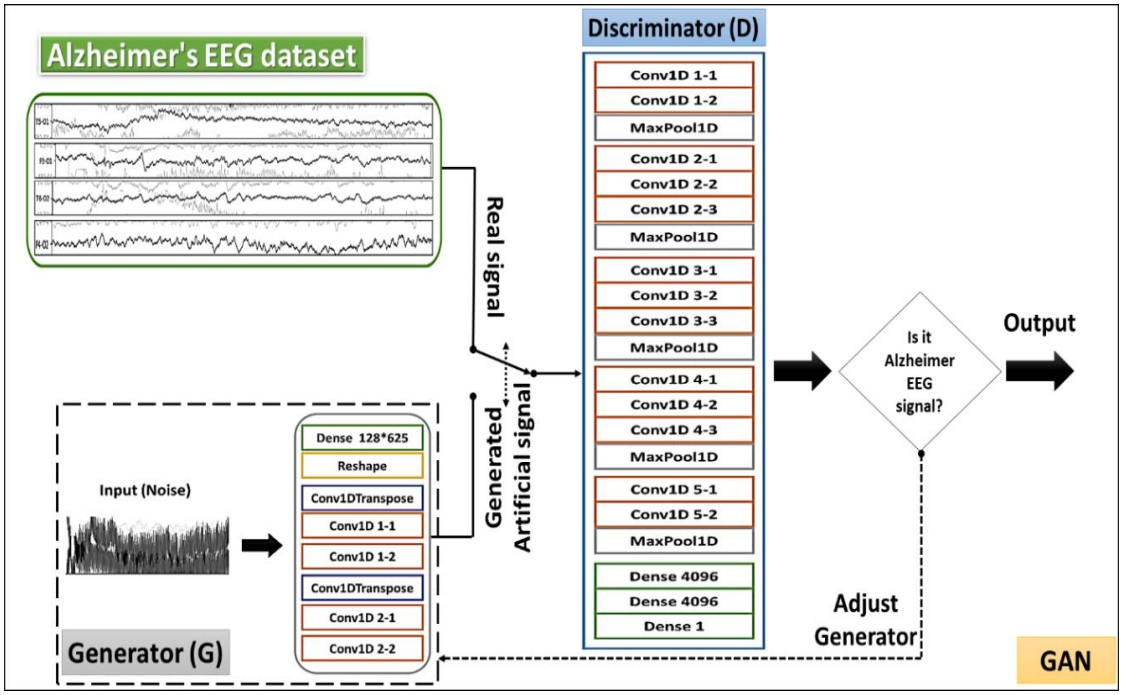

Figure 2. 1 The block diagram of the GAN model.

2.3. EVALUATION METRICS

Once Alzheimer's EEG dataset is processed, and the channels are divided, each channel is trained individually in 10000 epochs. The effectiveness of the system is evaluated using two metrics. These metrics were recently employed to evaluate the performance of GANs when generating EEG signals (Vo, Vishwanath, Srinivasan, Dutt, & Cao, 2022).

Spectral Entropy (SEN) is a statistical measure that evaluates the randomness or complexity of a signal's frequency spectrum. SEN quantifies the uniformity of signal energy distribution across different frequencies in the frequency domain. It is calculated by multiplying the power of each frequency with the logarithm of its power, and then summing up the products across all frequency bands (Vo et al., 2022).

$$H(x) = -\sum_{f=0}^{f_s/2} P(f)\log_2[P(f)] \qquad (11)$$

where P is the normalized power spectral density, and fs is the sampling frequency of signal x.

Reconstruction Error (REC) measures the differences between the values of an original signal and its reconstruction $\tilde{x}$ as (Vo et al., 2022):

$$REC = \left\| x_{1:T}^{q} - \tilde{x}_{1:T}^{q} \right\|_{1} \quad (12)$$

CHAPTER 3:

3. CLASSIFICATION SYSTEM

3.1. DATASET

3.1.1. EEG Dataset

The datasets are divided into two groups: Real Dataset (R) and Artificial dataset (AR). Real dataset is divided into Alzheimer dataset (RAD) and Healthy dataset (RH), which are a clinical EEG dataset collected from archival records at Temple University Hospital (TUH) named "TUH Abnormal EEG Corpus" (Obeid & Picone, 2016). The dataset was collected under the Declaration of Helsinki with the permission of the Temple University IRB. For Alzheimer dataset, set of 44 subjects (20 patients) were selected, and for Healthy dataset, set of 48 subjects (16 Healthy patients), as their diagnoses and patient histories contained Alzheimer's based on experts at the Temple University Hospital. The Artificial Dataset, on the other hand, consisted of the Artificial Alzheimer's Dataset (AAD). Artificial Alzheimer's EEG Dataset Generation (GAN Model) has been used to generate Artificial alzheimer dataset. A specialist from Kartal Dr. Lütfi Kırdar Hospital in Istanbul was involved in the evaluation step to ensure the inclusion of Alzheimer's disease in the dataset. This step is crucial to ensure the quality and accuracy of the dataset, as misclassification or incorrect labeling of samples can lead to biased results and incorrect conclusions in subsequent analysis. Table 3.1 illustrates the dataset used in classification system.

Table 3. 1 Summarizes the dataset used in classification system.

Type of dataset		**Gender**	**Age Range**	**Number of subjects**	**Number of patients**	**Duration (minute)**
Real dataset	**RAD**	Female	59 - 92	25	13	269.9 m
		Male	53 - 93	19	7	278.5 m
	RH	Female	22 - 81	27	10	365.8 m
		Male	21 - 70	21	6	252.2 m
Artificial dataset	**AAD**	-	-	1	-	151.6 m

As well, the MNE package has preprocessed the dataset by removing interference and eliminating ocular artefacts and electromyographic signals (EMG) (Gramfort et al., 2014). The EEG signals have also been manually examined to ensure that they contain no unwanted signals.

3.1.2. Data Augmentation

Data augmentation is a technique used to increase the size and diversity of a training dataset by creating new samples from existing data. There are several techniques for data augmentation such as flipping and rotation, cropping and resizing, color jittering, adding noise, and synthetic generation (Maharana, Mondal, & Nemade, 2022). In our work, random noise has been used to increase the size and diversity of the training dataset, which can improve the ability of the model to generalize to new data and reduce overfitting. The processed EEG channels were organized in segments of 1s equal to 17300 sample in Healthy Dataset (RH), 8650 sample in Alzheimer Dataset (RAD), 8650 sample in Artistical Dataset (AAD), and 17300 in Augmented data (AUG). Segmentation helps to break down the data into smaller, more manageable chunks, which can make it easier to analyze and process. Additionally, it can help to improve the accuracy of the classification model by allowing it to capture more detailed temporal information about the EEG signals.

3.1.3. Examination Sets

The amount of dataset can have a significant impact on the performance of classification models. Generally, increasing the amount of training data tends to improve the accuracy of the model, as it provides more examples for the model to learn from and helps it to generalize better to new data. Thus, examination sets were implemented into six groups; These groups have been chosen experimentally, starting with a fewer value, and increasing until the network resolution changed significantly. Table 3.2 is summarized examination sets used in this study.

Table 3. 2 The examination sets for classification AD.

Examination Sets	Type of data				Total (sample)
	RH	RAD	AAD	AUG	
RAD (100%)	8650	8650	0	0	17300 s
AAD (100%)	8650	0	8650	0	17300 s
RAD (100%) + AAD (25%)	10813	8650	2163	0	21626 s
RAD (100%) + AAD (50%)	12975	8650	4325	0	25950 s
RAD (100%) + AAD (100%)	17300	8650	8650	0	34600 s
RAD (100%) + AAD (100%) + AUG	17300	8650	8650	17300	51900 s

3.2. CLASSIFICATION MODELS

3.2.1. Visual Geometry Group (VGG16)

VGG16 has been used for classification Alzheimer's EEG signals. Our modified VGG16 model is designed with sixteen layers, starting with thirteen *Conv1D layers* that have filter sizes of 64, 128, 256, and 512, and kernel sizes of 3, 5, and 7. Additionally, we have incorporated five *MaxPool layers* with two filters of stride two between the convolution layers to reduce the dimensionality of the output. To ensure efficient training, we have chosen rectified linear activation (*ReLU*) as the activation function for the convolutional layers. The final three layers of our VGG16 model are *dense*, consisting of two layers of 4096 units that use ReLU as the activation function and an output layer of one unit that uses sigmoid as the activation function. We use the *Adam* optimizer with a learning rate of 0.0001 and a momentum of 0.5 for training our VGG16 model. For clarity, a summary of our VGG16 model architecture is provided in Figure 3.1.

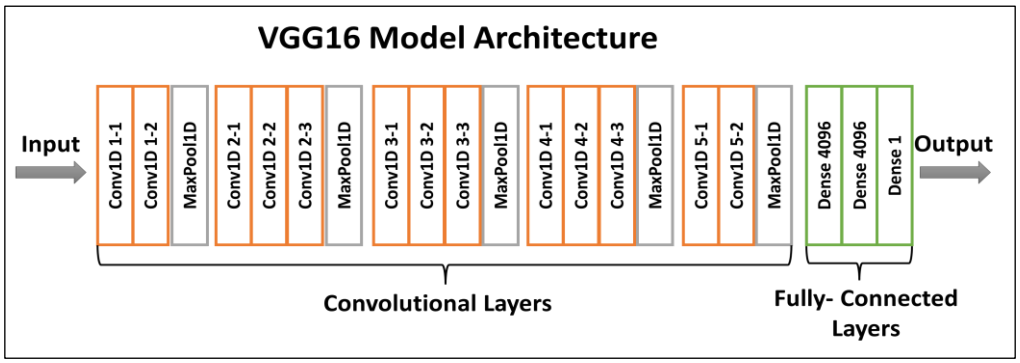

Figure 3. 1 VGG16 model architecture of our model.

3.2.2. Long Short-Term Memory (LSTM)

LSTM has been used for classification Alzheimer's EEG signals. LSTM model consists of seven layers starting with the *dense layer*, with enough nodes to represent a low-resolution version of the output signal. The core of the recurrent neural network consists of two cascaded *LSTM layers*. Each *LSTM layer* is followed by a dropout layer that randomly discards some of the input data. Finally, there are two fully-connected layers (*dense layer*) of size (64, 2) using RELU as the activation function and the model's output layer is using SoftMax as the activation function. The *Adam* optimizer with a learning rate of 0.0001 and a momentum of 0.2 is utilized in LSTM models. Figure 3.2 provides a summary of our LSTM model architecture.

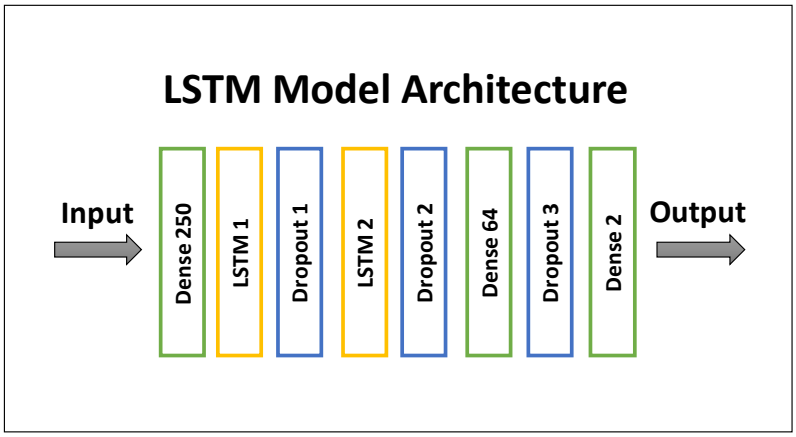

Figure 3. 2 LSTM model architecture of our model.

3.2.3. Milit-Layer Perceptron (MLP)

In our work, we utilized an MLP architecture comprising of 11 hidden layers, each with 4096 units. The activation function employed between these layers was rectified linear activation (*ReLU*) with a slope of 0.2, which has been shown to be effective in enhancing the performance of deep neural networks. To optimize the model's weights, we used the *Adam* optimizer with a low learning rate of 0.000001 and a momentum of 0.5, which helped in achieving faster convergence during the training process. Figure 3.3 provides a summary of our MLP model architecture.

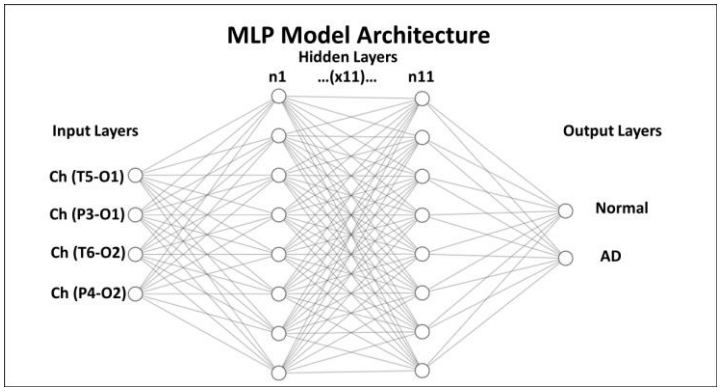

Figure 3. 3 MLP model architecture of our model.

3.2.4. Transformer

In our work, an encoder has been used for classification Alzheimer's EEG signals. we utilized a Transformer model with two encoder layers. The model's hyperparameters included four self-attention heads with a size of 512. To achieve a minimal loss during the model training process, we combined the Root Mean Squared Propagation optimizer (*RMSprop*) with a learning rate of 10-6. This combination of hyperparameters allowed the model to efficiently map input sequences to continuous representations and generate output sequences with high accuracy. Figure 3.4 provides a summary of our Transformer model architecture.

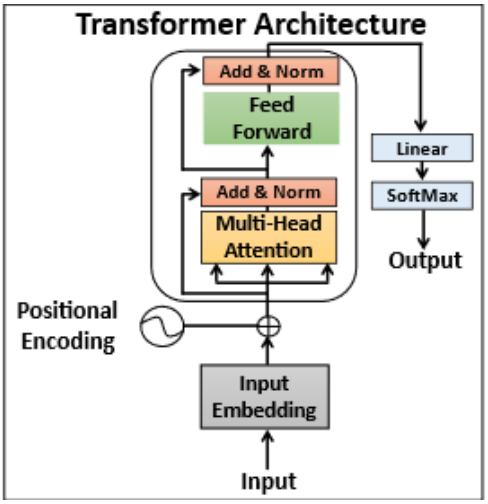

Figure 3. 4 Transformer model architecture of our model.

In this chapter, we have been described the steps involved in developing a classification system for Alzheimer's disease diagnosis using EEG datasets. These steps are illustrated in Figure 3.5 and include Dataset, Preprocessing, Examination Sets, and Classification Models. Firstly, the Dataset step involves collecting the EEG recordings from patients with Alzheimer's disease as well as healthy individuals. Next, the Preprocessing step is used to analyze and process the dataset in order to remove any noise and interference from the brain patterns. This step involves techniques such as filtering, artifact removal, and normalization. In addition, data augmentation techniques such as adding random noise have been used to increase the size and diversity of the training dataset. The Examination Sets step involves dividing the preprocessed data into several sets to examine the performance of the classification models. Finally, the Classification Models step involves using various deep learning models such as CNN, RNN, MLP, and Transformer to classify the obtained data. Overall, by following these steps, it is possible to develop a reliable and accurate classification system for Alzheimer's disease diagnosis using EEG recordings.

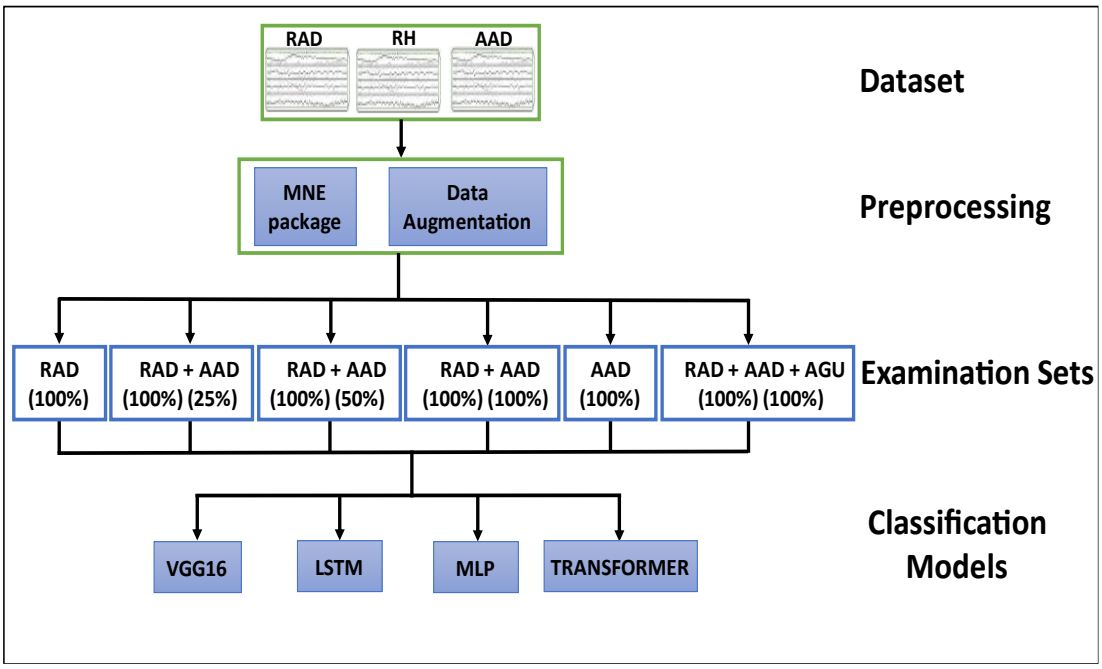

Figure 3. 5 The block diagram of proposed models in classification AD.

3.3. EVALUATION METRICS

Evaluation metrics play a crucial role in assessing the performance of classification models. In our study, we have chosen the following evaluation metrics for assessing the performance of our classification models:

3.3.1. Cross-Validation

Since our dataset is limited, Cross-validation is used to evaluate the performance of classification models. It involves dividing the original dataset into two or more subsets, a training set and a validation set. The model is trained on the training set, and its performance is evaluated on the validation set. There are different types of cross-validation techniques, k-fold cross-validation algorithm has been used (Refaeilzadeh, Tang, & Liu, 2009). It involves dividing the original dataset into *K* equally sized subsets or folds. The model is then trained on *K-1* of the folds and tested on the remaining fold. This process is repeated K times, with each fold being used as the test set once.

In our work, 10-fold cross-validation has been utilized, which all processed dataset has been transmitted to the 10-fold cross-validation. Next, samples were divided into a 90% subset for the training set and a 10% of subset for the validation set. This process is done 10 times, so classifier could train to all samples. After that, the performance and the accuracy of the model will be calculated by the following equation (13).

$$Accuracy = \frac{A_{Total}}{10} * 100 \qquad (13)$$

Where A_{Total} the total number of accuracies for each set. The resulting accuracy score provides a robust estimate of the model's performance, considering the variability of the data and the different subsets used for training and validation.

3.3.2. Matthews Correlation Coefficient (MCC)

The Matthews Correlation Coefficient (MCC) is a measure commonly used to assess the quality of binary (two-class) classification models. It was introduced by Brian Matthews in 1975 (Matthews, 1975). The MCC quantifies the difference or

discrepancy between the predicted values and the actual values and is analogous to the chi-square statistic for a 2 x 2 contingency table. It can be calculated by equation 14.

$$MCC = \frac{TN \times TP - FN \times FP}{\sqrt{(TP + FP)(TP + FN)(TN + FP)(TN + FN)}} \qquad (14)$$

where *TP* represents true positives, *TN* represents true negatives, *FP* represents false positives, and *FN* represents false negatives.

The MCC ranges from -1 to +1, with +1 indicating a perfect prediction, 0 indicating a random prediction, and -1 indicating a completely inverse prediction. It can be interpreted as a measure of the correlation between the predicted and actual binary classifications.

3.3.3. Sensitivity, Specificity and Precision

Sensitivity, also known as Recall, measures the ability of a model to correctly identify positive instances. It calculates the proportion of true positives out of all actual positive instances (Raschka, 2014). It can be calculated by equation 15.

$$SEN = \frac{TP}{TP + FN} \qquad (15)$$

where *TP* represents true positives and *FN* represents false negatives.

Specificity measures the ability of a model to correctly identify negative instances. It calculates the proportion of true negatives out of all actual negative instances (Raschka, 2014). It can be calculated by equation 16.

$$SPC = \frac{TN}{TN + FP} \qquad (16)$$

where TN represents true negatives and FP represents false positives.

Precision, also known as Positive Predictive Value, measures the ability of a model to avoid false positives. It calculates the proportion of true positives out of all positive predictions made by the model (Raschka, 2014). It can be calculated by equation 17.

$$PPV = \frac{TP}{TP + FP} \qquad (17)$$

where *TP* represents true positives and *FP* represents false positives.

CHAPTER 4

4. RESULTS AND DISCUSSION

4.1. BENCHMARK RESULTS OF DATASET GENERATION SYSTEM

In the dataset generation system, we proposed a model to create artificial EEG signals for Alzheimer's disease. The primary motivation is the difficulty accessing real datasets in training the networks for diagnosis. Generative Adversarial Network (GAN) is deployed to model the disease and generate artificial datasets for researchers to employ. Two models (GANAlzh-1, GANAlzh-2) have been selected from the generated epochs. Table 4.1 presents the performance of the proposed models in generating Alzheimer's EEG signals. Both GANAlzh-1 and GANAlzh-2 models achieve significantly lower REC and SEN differences. The performance of GANAlzh-1 is better than GANAlzh-2 since SEN differences are lower (0.049) than those of GANAlzh-2 (0.086). However, the results show that both models are more effective at capturing Alzheimer's EEG signal features in the time and frequency domains.

The channel frequency domains are also examined to determine the similarity between the real and artificial channels. Figure 4.1 represents how closely real and artificial signals resemble each other in their frequency as the average number of peaks in ten seconds. The real signal has 67 peaks, while the artificial signal has 63, reinforcing the model's efficacy in generating the signals associated with Alzheimer's disease.

Table 4. 1 Performances of GANALZH-1 and GANALZH-2 models in measuring spectral entropy and reconstruction tasks.

	REC	**SEN**
Alzheimer Dataset		0.487 ± 0.063
GANAlzh-1	0.043 ± 0.024	0.438 ± 0.056
GANAlzh-2	0.044 ± 0.014	0.401 ± 0.043

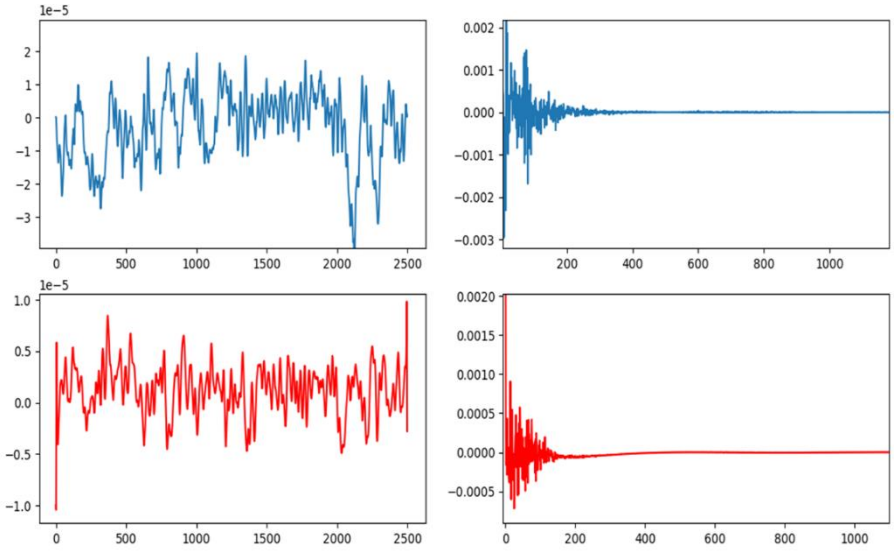

Figure 4. 110-second of the channel (T5-O1) in Real and Artificial EEG recording for Alzheimer's EEG signal. The blue graphs are for Real EEG recording, while the red is for artificial.

4.2. BENCHMARK RESULTS OF CLASSIFICATION SYSTEM

As discussed previously, two types of EEG datasets (Real Dataset (R) and Artificial dataset (AR)) were used in this study. Real datasets were recorded from 44 Alzheimer subjects (RAD) and 48 Healthy subjects (RH), while Artificial dataset was generated from Artificial Alzheimer's EEG Dataset Generation. In order to improve signal-to-noise ratio, the dataset has been reprocessed by using the MNE package for removing the noise and unwanted signals. Then one of the augmentation techniques has been used to increase the amount of dataset. Finally, four types of classifiers (VGG16, LSTM, MLP, and Transformer) have been employed for distinguishing EEG signals corresponding to their group and the classification accuracies have been computed and compared with each other. Each model was trained 100, 150, 200, 250, 300 epochs respectively to see when the system reached a cut off state. We have found that 300 epochs are suitable for the models as figure 4.2 shows the accuracy and the loss of the trained models. Furthermore, according to the amount of EEG dataset, six examinations sets have been investigated as following:

- ✓ Real dataset (RAD (100%))
- ✓ Artificial dataset (AAD (100%))
- ✓ Full Real dataset and quarter of Artificial dataset (RAD (100%) +AAD (25%))
- ✓ Full Real dataset and half of Artificial dataset (RAD (100%) +AAD (50%))
- ✓ Full Real dataset and full of Artificial dataset (RAD (100%) +AAD (100%))
- ✓ Full Real dataset, full of Artificial dataset, and augmented data (RAD (100%) +AAD (100%) +AUG)

Sections III-A through III-F provide classification results for each examination set, demonstrating the performance of each classifier and the effectiveness of using augmented and artificial datasets to improve classification accuracy.

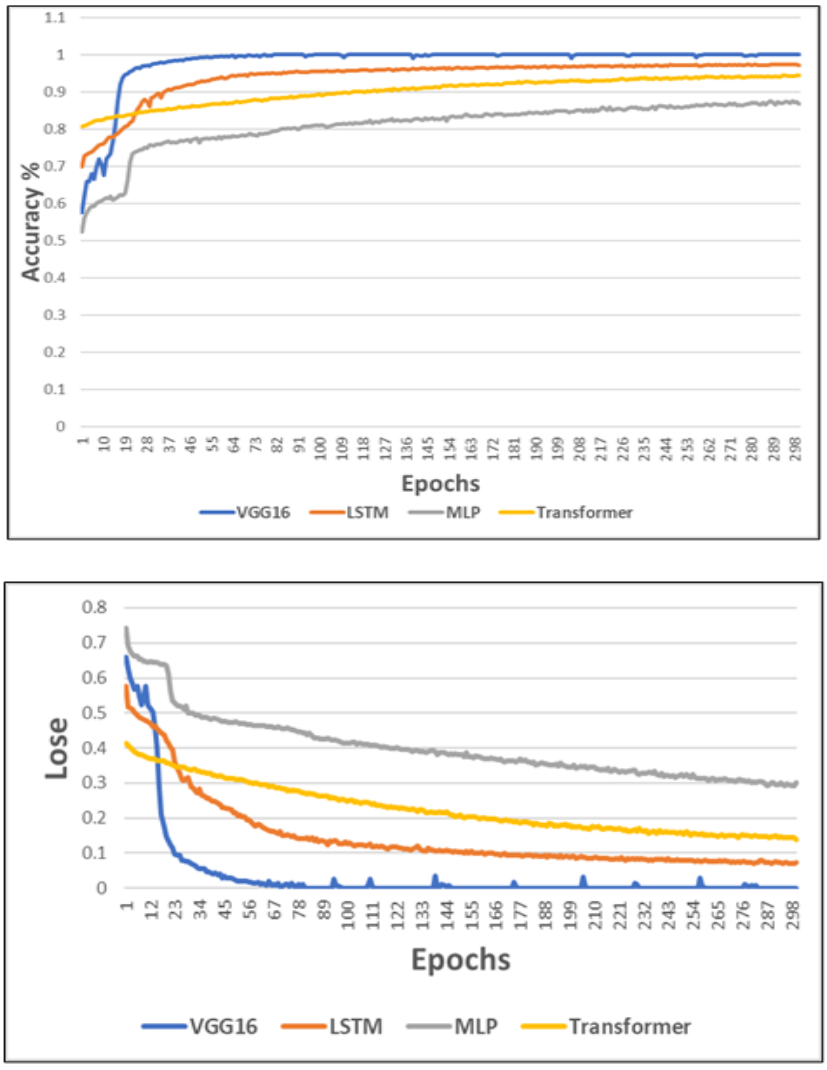

Figure 4. 2 a) Plot of the training accuracy in training epochs for each classifier. b) Plot of the training loss in training epochs for each classifier.

4.2.1. Real dataset (RAD (100%))

In this section, the set of 8650 Real Alzheimer samples forms the class “AD” has been combined with the set of 8650 healthy samples forms the class "Normal". The average classification accuracy, MCC, Sensitivity, Specificity and Precision among four classifiers for the first examination sets is shown in Table 4.2. Also, Figure 4.3.a illustrates the confusion matrices for all classifiers and provides the average accuracy. The VGG16 classifier showed the best performance, and the accuracy is 97.17 % as can be observed.

Table 4. 2 The average classification accuracy, MCC, Sensitivity, Specificity and Precision in Real dataset.

Ex. Set	**RAD (100%)**									
Classifier Model	**Accuracy**		**MCC**		**Sensitivity**		**Specificity**		**Precision**	
	Mean	**StD**	**Mean**	**StD**	**Mean**	**StD**	**Mean**	**StD**	**Mean**	**StD**
VGG16	97.17 %	± 0.41	0.919	± 0.03	95.94 %	± 0.22	95.94 %	± 0.22	95.90 %	± 0.02
LSTM	95.89 %	± 0.01	0.917	± 0.04	94.95 %	± 0.19	94.95 %	± 0.19	94.80 %	± 0.03
MLP	87.86 %	± 0.02	0.756	± 0.03	87.90 %	± 0.03	87.95 %	± 0.10	87.70 %	± 0.04
Transformer	74.23 %	± 0.04	0.510	± 0.05	76.81 %	± 0.08	76.67 %	± 0.07	74.40 %	± 0.15

4.2.2. Artificial dataset (AAD (100%))

In this section, the set of 8650 Artificial Alzheimer samples forms the class “AD” has been combined with the set of 8650 healthy samples forms the class "Normal". The average classification accuracy, MCC, Sensitivity, Specificity and Precision among four classifiers for the first examination sets is shown in Table 4.3. Figure 4.3.b illustrates the confusion matrices for all classifiers and provides the average accuracy. It can be seen that the artificial dataset and real dataset gave approximate accuracy results, which indicates the efficiency of the Artificial Alzheimer’s EEG Dataset Generation. Also, The VGG16 classifier showed the best performance, and the accuracy is 98.10 % as can be observed.

Table 4. 3 The average classification accuracy, MCC, Sensitivity, Specificity and Precision in Artificial dataset.

Ex. Set	AAD (100%)									
Classifier Model	Accuracy		MCC		Sensitivity		Specificity		Precision	
	Mean	StD	Mean	StD	Mean	StD	Mean	StD	Mean	StD
VGG16	98.10 %	± 0.94	0.910	± 0.01	98.12 %	± 0.09	97.94 %	± 0.10	98.90 %	± 0.01
LSTM	94.39 %	± 0.03	0.964	± 0.12	96.45 %	± 0.02	96.78 %	± 0.09	97.80 %	± 0.02
MLP	86.11 %	± 0.05	0.785	± 0.14	88.57 %	± 0.07	88.44 %	± 0.04	86.47 %	± 0.08
Transformer	76.67 %	± 0.07	0.657	± 0.20	76.74 %	± 0.08	76.67 %	± 0.07	75.77 %	± 0.09

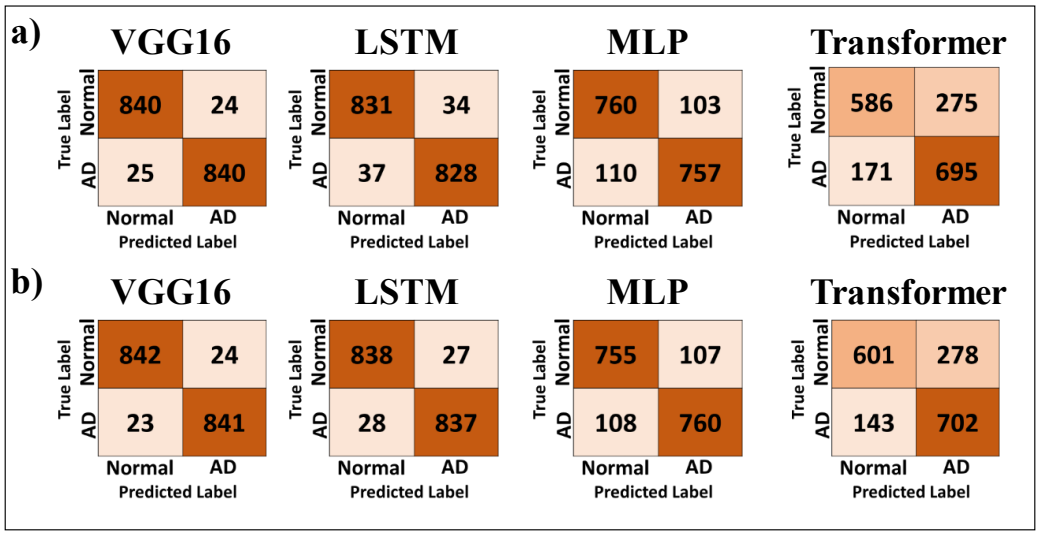

Figure 4. 3 a) Confusion matrices for all classifiers in Real dataset set. b) Confusion matrices for all classifiers in Artificial dataset set.

4.2.3. Full Real dataset and quarter of Artificial dataset (RAD (100%) +AAD (25%))

In this section, the set of 8650 Real Alzheimer samples and 2163 Artificial Alzheimer samples forms the class “AD” has been combined with the set of 10813 healthy samples forms the class "Normal". The average classification accuracy, MCC, Sensitivity, Specificity and Precision among four classifiers for the first examination sets is shown in Table 4.4. The confusion matrices for all classifiers are illustrated in Figure 4.4.a. We also notice that there is a significant improvement in accuracy in MLP and Transformer Models, and this indicates that it needs more dataset to be able

to learn. As well, the VGG16 classifier showed the best performance, and the accuracy is 97.30 % as can be observed.

Table 4. 4 The average classification accuracy, MCC, Sensitivity, Specificity and Precision in Full Real dataset and quarter of Artificial dataset.

Ex. Set	RAD (100%) +AAD (25%))									
Classifier Model	Accuracy		MCC		Sensitivity		Specificity		Precision	
	Mean	StD	Mean	StD	Mean	StD	Mean	StD	Mean	StD
VGG16	97.30 %	± 1.37	0.922	± 0.02	96.12 %	± 0.02	96.25 %	± 0.05	96.08 %	± 0.03
LSTM	96.04 %	± 0.01	0.926	± 0.02	96.32 %	± 0.02	96.58 %	± 0.04	96.56 %	± 0.02
MLP	89.03 %	± 0.02	0.781	± 0.03	89.09 %	± 0.13	89.84 %	± 0.11	89.04 %	± 0.03
Transformer	77.37 %	± 0.03	0.564	± 0.04	79.05 %	± 0.07	79.57 %	± 0.08	77.43 %	± 0.12

4.2.4. Full Real dataset and half of Artificial dataset (RAD (100%) +AAD (50%))

In this section, the set of 8650 Real Alzheimer samples and 4325 Artificial Alzheimer samples forms the class “AD” has been combined with the set of 12975 healthy samples forms the class "Normal". The average classification accuracy, MCC, Sensitivity, Specificity and Precision among four classifiers for the first examination sets is shown in Table 4.5. The confusion matrices for all classifiers are illustrated in Figure 4.4.b. It has seen a sustained accuracy improvement in the MLP and Transformer models. As well, the VGG16 classifier showed the best performance, and the accuracy is 97.51% as can be observed.

Table 4. 5 The average classification accuracy, MCC, Sensitivity, Specificity and Precision in Full Real dataset and half of Artificial dataset.

Ex. Set	RAD (100%) +AAD (50%)									
Classifier Model	Accuracy		MCC		Sensitivity		Specificity		Precision	
	Mean	StD	Mean	StD	Mean	StD	Mean	StD	Mean	StD
VGG16	97.51 %	± 0.02	0.950	± 0.01	97.51 %	± 0.05	97.25 %	± 0.05	97.51 %	± 0.04
LSTM	96.68 %	± 0.04	0.959	± 0.07	96.26 %	± 0.05	96.28 %	± 0.04	96.56 %	± 0.02
MLP	90.50 %	± 0.03	0.789	± 0.16	89.48 %	± 0.12	89.65 %	± 0.10	89.46 %	± 0.01
Transformer	82.20 %	± 0.08	0.646	± 0.07	82.46 %	± 0.03	82.57 %	± 0.04	82.20 %	± 0.04

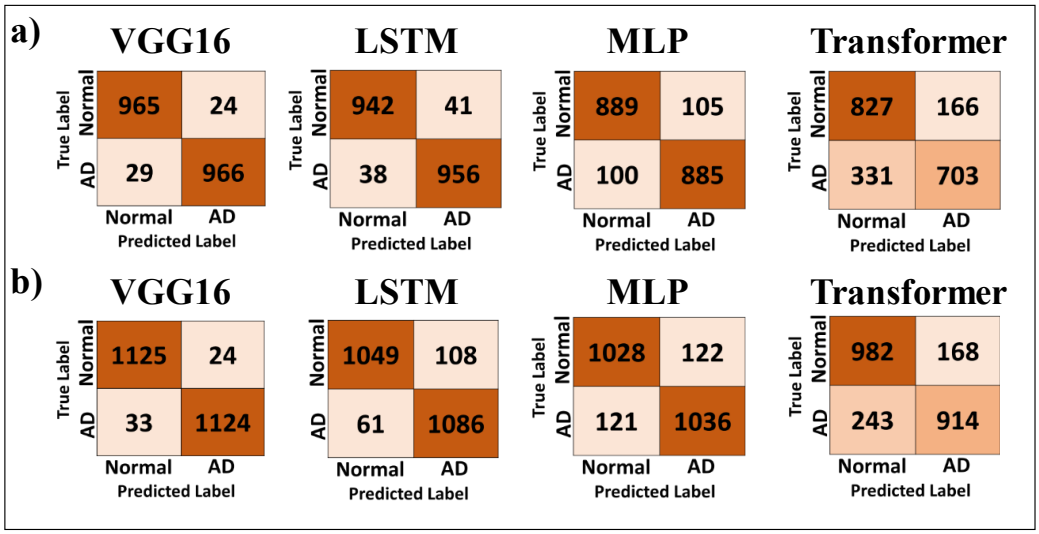

Figure 4. 4 a) Confusion matrices for all classifiers in in Full Real dataset and quarter of Artificial dataset set. b) Confusion matrices for all classifiers in Full Real dataset and half of Artificial dataset set.

4.2.5. Full Real dataset and full of Artificial dataset (RAD (100%) +AAD (100%))

In this section, the set of 8650 Real Alzheimer samples and 8650 Artificial Alzheimer samples forms the class “AD” has been combined with the set of 17300 healthy samples forms the class "Normal". The average classification accuracy, MCC, Sensitivity, Specificity and Precision among four classifiers for the first examination sets is shown in Table 4.6. The confusion matrices for all classifiers are illustrated in Figure 4.5.a. The results showed that, while there was an improvement in accuracy in MLP and Transformer models, it was not enough to achieve good results due to the limited amount of data available for training and testing the classifiers. The VGG16 classifier continued to exhibit the best performance, achieving an accuracy of 97.89%.

Table 4. 6 The average classification accuracy, MCC, Sensitivity, Specificity and Precision in Full Real dataset and full Artificial dataset.

Ex. Set	RAD (100%) +AAD (100%)									
Classifier Model	Accuracy		MCC		Sensitivity		Specificity		Precision	
	Mean	StD	Mean	StD	Mean	StD	Mean	StD	Mean	StD
VGG16	97.89 %	± 0.03	0.968	± 0.05	97.90 %	± 0.08	97.95%	± 0.04	97.90 %	± 0.08
LSTM	97.39 %	± 0.03	0.962	± 0.06	97.66 %	± 0.04	97.50 %	± 0.03	97.56 %	± 0.05
MLP	92.10 %	± 0.01	0.814	± 0.07	90.70 %	± 0.09	90.86 %	± 0.10	90.70 %	± 0.01
Transformer	85.25 %	± 0.05	0.712	± 0.08	85.93 %	± 0.08	85.57 %	± 0.04	85.31 %	± 0.09

4.2.6. Full Real dataset, full of Artificial dataset, and Augmented dataset (RAD (100%) +AAD (100%) +AUG)

In this section, the set of 8650 Real Alzheimer samples, 8650 Artificial Alzheimer samples, and 8650 Augmented samples forms the class “AD” has been combined with the set of 17300 healthy samples and 8650 Augmented samples forms the class "Normal". The average classification accuracy, MCC, Sensitivity, Specificity and Precision among four classifiers for the first examination sets is shown in Table 4.7. The confusion matrices for all classifiers are illustrated in Figure 4.5.b. The results of the evaluation demonstrated that the addition of data led to an improvement in the performance of all models. In particular, the results obtained from the transformer model were found to be promising. Furthermore, the VGG16 model achieved the highest result among all the classifiers, with an accuracy of 99.67%.

Table 4. 7 The average classification accuracy, MCC, Sensitivity, Specificity and Precision in Full Real dataset, full Artificial dataset, and Augmented dataset.

Ex. Set	RAD (100%) +AAD (100%) +AUG									
Classifier Model	Accuracy		MCC		Sensitivity		Specificity		Precision	
	Mean	StD	Mean	StD	Mean	StD	Mean	StD	Mean	StD
VGG16	99.67 %	± 0.02	0.982	± 0.01	99.51 %	± 0.06	99.39%	± 0.09	99.25 %	± 0.02
LSTM	99.35 %	± 0.04	0.981	± 0.04	99.42 %	± 0.09	99.28 %	± 0.03	99.14 %	± 0.08
MLP	95.52 %	± 0.05	0.898	± 0.01	95.12 %	± 0.07	95.07 %	± 0.08	95.08 %	± 0.05
Transformer	96.63 %	± 0.08	0.904	± 0.12	96.45 %	± 0.03	96.42 %	± 0.02	96.31 %	± 0.09

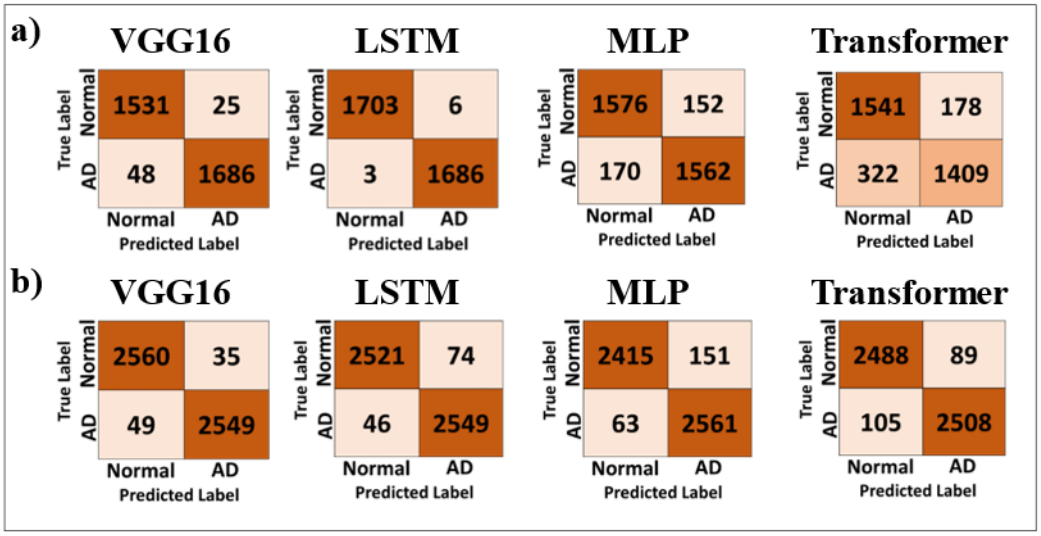

Figure 4. 5 a) Confusion matrices for all classifiers in full Real dataset and full Artificial dataset set. b) Confusion matrices for all classifiers in Full Real dataset, full Artificial dataset, and Augmented dataset set.

4.3. DISCUSSION

In the dataset generation system, the proposed models have achieved high accuracy, which generated slow waves at 5-7 Hz and 60 microvolts amplitude in the three channels ($(T_5\text{-}O_1)$, $(T_6\text{-}O_2)$, $(P_4\text{-}O_2)$). However, sometimes the frequency range increases from 7 to 10 Hz in the $P_3\text{-}O_1$ channel when the model generates longer sessions. The generated signals were evaluated based on the observations from our corpus and a neuroscientist from the EEG department at Kartal Dr. Lütfi Kirdar hospital in Istanbul, Turkiye. Figure 4.6. a is an example of a real Alzheimer's EEG signal of a 73-year-old woman with a history of Alzheimer's. We have observed that Alzheimer's disease affects the occipital and temporal regions of the brain ($(T_5\text{-}O_1)$, $(P_3\text{-}O_1)$, $(T_6\text{-}O_2)$, $(P_4\text{-}O_2)$), which decrease the power of frequency and make them between 4-8 Hz. Figure 4.6. b is an artificial Alzheimer's EEG signal generated by the proposed model. EEG recordings usually contain noise such as interference (50Hz, 60Hz), ocular artefacts, and (EMG) that require preprocessing before they can be used. Since our models can also generate noise-free signals, we can eliminate the preprocessing before the data is utilized for classification purposes.

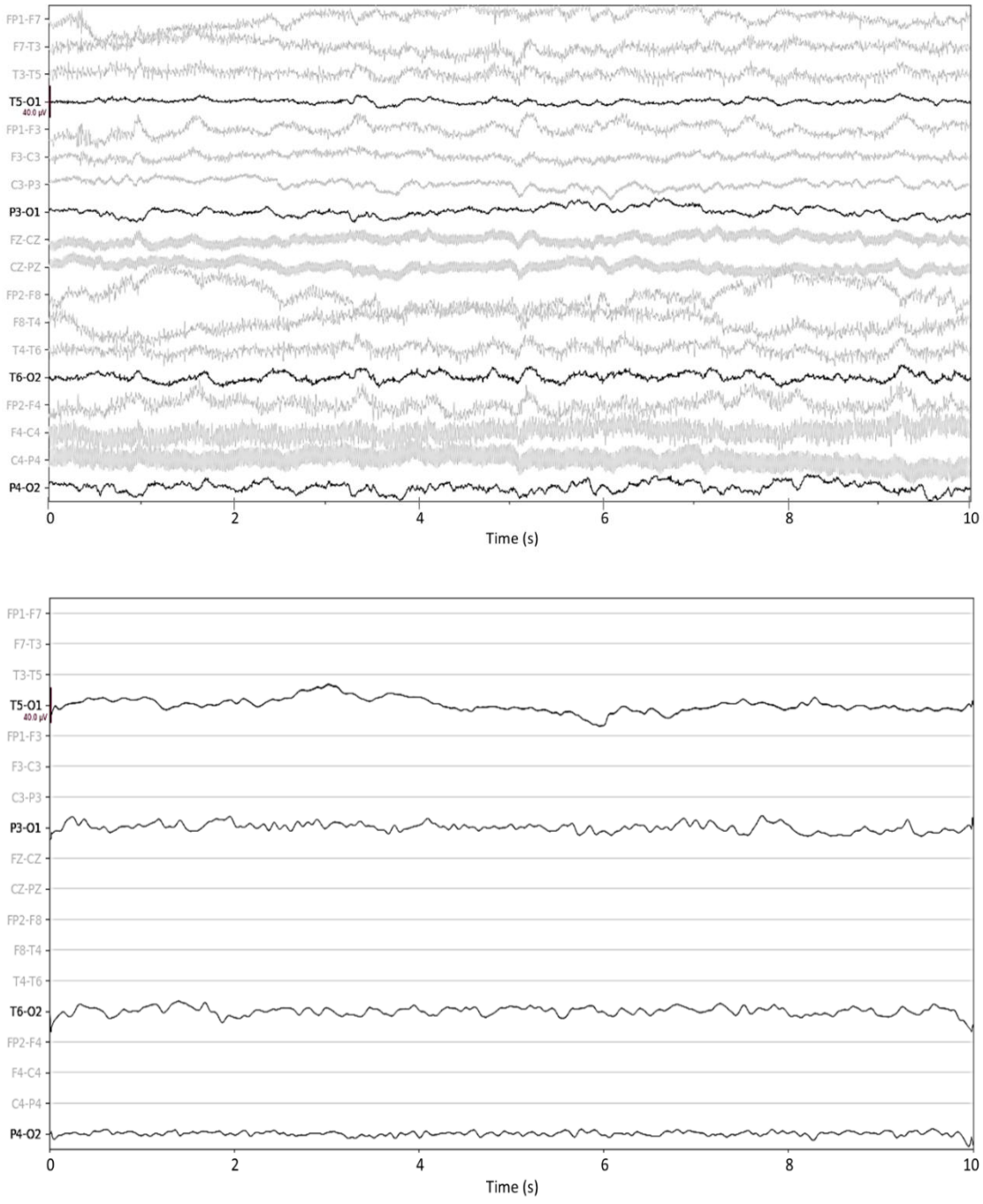

Figure 4. 6 a) 10-second from 20-minute EEG recording for Alzheimer's EEG signal of a 73-year woman with a history of Alzheimer's. b) 10-second from 20-minute Artificial EEG recording for Alzheimer's EEG signal.

In classification system, table 4.8 presents the best classification accuracy of VGG16, LSTM, MLP and Transformer models. From the table, it can be seen the performed experiments have shown that the VGG16, LSTM, MLP and Transformer models can recognize subjects with AD, from the dataset used for the tests, with a high accuracy 99.98 %, 99.76 %, 97.58 %, and 97.34 % respectively. In VGG16 model, we notice that the performance of the model improves slightly when the amount of dataset is increased, as well in LSTM model. However, we observe that the performance of the MLP and Transformer models significantly improves when the amount of dataset is increased, and this indicates that it needs more dataset to be able to learn and enhance their performance. Also, there is a slight difference between the models' performance when tested on real (RAD 100%) versus artificial (AAD 100%) datasets. This discrepancy is due to the Artificial Alzheimer's EEG Dataset Generation's ability to generate noise-free signals for AD. This noise-free dataset makes it easier for the models to recognize AD, leading to higher classification accuracy.

Table 4. 8 The best classification accuracy for all classifiers in each examination set.

Classifier / **Examination Sets**	**VGG16**	**LSTM**	**MLP**	**Transformer**
RAD (100%)	98.30 %	97.21 %	89.71 %	78.61 %
AAD (100%)	99.27 %	98.85 %	90.17 %	80.77 %
RAD (100%) + AAD (25%)	98.47 %	97.63 %	90.13 %	80.32 %
RAD (100%) + AAD (50%)	98.89 %	98.04 %	90.85 %	83.53 %
RAD (100%) + AAD (100%)	99.24 %	98.23 %	93.71 %	88.38 %
RAD (100%) + AAD (100%) + AUG	99.98 %	99.76 %	97.58 %	97.34 %

Our study showcases the exceptional performance of machine learning models in accurately classifying EEG signals in Alzheimer's disease. Specifically, our approach using the CNN model achieved an unprecedented classification accuracy of 99.98%, surpassing the results reported in previous studies such as *Morabito et al.* (Morabito et al., 2016), *Ieracitano et al.* (Ieracitano et al., 2020a) and *Fouladi et al.* (Fouladi et al., 2022) who achieved maximum accuracy of 85%, 85.78%, and 92%, respectively using a convolutional neural network classifier. Moreover, our RNN model also exhibited impressive classification accuracy of 99.76%, which is significantly higher than the results reported in other studies such as *Alvi et al.* (Alvi et al., 2022) and *Alessandrini et al* (Alessandrini et al., 2022), which identified

Alzheimer's patterns with accuracy rates of 96.41% and 93.5%, respectively. Moreover, our MLP model also demonstrated remarkable results with a classification accuracy of 97.58%, surpassing Ieracitano's study (Ieracitano et al., 2020b) which achieved 97%.

Furthermore, machine learning models are also good tool in the classification of AD as indicated by previous studies (AlSharabi et al., 2022; Cassani et al., 2017). *Alsharabi et al.* (AlSharabi et al., 2022) approaches achieved remarkable results and best classification accuracy achieved in KNN classifier achieved which is 99.98%. This result is similar to that achieved by VGG16 model. Also, Transformer also showed promising results in classification Alzheimer's disease which our model achieved 97.34 %. Although it has lower results than previous models, because it needs a larger amount of data.

Our findings suggest that deep learning models can be a valuable asset for improving the accuracy and efficiency of Alzheimer's diagnosis. The ability of these models to detect aberrant brain patterns associated with Alzheimer's disease has shown promise in aiding early diagnosis and improving patient prognosis. Additionally, the high accuracy achieved by these models highlights their potential as reliable and cost-effective diagnostic tools. Finally, our study emphasizes the importance of machine learning models in advancing the field of Alzheimer's disease diagnosis and treatment. We believe that the continued development and refinement of these models can lead to improved accuracy and efficacy in diagnosing and treating this disease.

4.4. CONCLUSION

Deep learning has emerged as a powerful tool for EEG feature analysis, enabling us to better understand and detect patterns of neurological disorders, including Alzheimer's disease. This work proposed generating artificial Alzheimer's EEG signals using generative adversarial networks. We can leverage GANs to generate artificial Alzheimer's EEG signals from noise. It allows us to create high-accuracy classification models and expand the scope of our research. Based on the results, our method is characterized effectively in generating Alzheimer's signals. The method shows potential for new generative applications in neuroscience and neurology.

Furthermore, our proposed models, Convolutional Neural Network (CNN), Recurrent Neural Network (RNN), Multi-Layer Perceptron (MLP) and Transformer, have been able to achieve accurate classification with a high accuracy 99.98 %, 99.76 %, 97.58 %, and 97.34 % respectively.

When comparing our results with those of similar past research, our approach has demonstrated significantly higher diagnosis accuracy. This indicates that our approach is more effective in accurately identifying Alzheimer's disease patients from EEG signals.

4.5. FUTURE WORK

We acknowledge that there is always room for improvement in the field of EEG signal analysis, and we will continue to explore new techniques and approaches to further enhance the accuracy and reliability of our model. Future directions include developing methods that generate Alzheimer's signals at all stages with the possibility of controlling the properties of the generated signal. It can contribute to the development of more accurate and efficient diagnostic tools for Alzheimer's disease.

REFERENCES

Ajit, A., Acharya, K., & Samanta, A. (2020). *A review of convolutional neural networks.* Paper presented at the 2020 international conference on emerging trends in information technology and engineering (ic-ETITE).

Al-Jumeily, D., Iram, S., Vialatte, F.-B., Fergus, P., & Hussain, A. J. T. s. w. j. (2015). A novel method of early diagnosis of Alzheimer's disease based on EEG signals. *2015*.

Alessandrini, M., Biagetti, G., Crippa, P., Falaschetti, L., Luzzi, S., & Turchetti, C. J. S. (2022). EEG-Based Alzheimer's disease recognition using robust-PCA and LSTM recurrent neural network. *22*(10), 3696.

AlSharabi, K., Salamah, Y. B., Abdurraqeeb, A. M., Aljalal, M., & Alturki, F. A. J. I. A. (2022). EEG signal processing for Alzheimer's disorders using discrete wavelet transform and machine learning approaches. *10*, 89781-89797.

Alvi, A. M., Siuly, S., & Wang, H. J. I. T. o. E. T. i. C. I. (2022). A long short-term memory based framework for early detection of mild cognitive impairment from EEG signals.

Alzheimer's, A. s. A. J., & dementia. (2022). 2022 Alzheimer's disease facts and figures. *15*(3), 321-387.

Alzheimer's Disease Fact Sheet. (July 08, 2021, Feb 08, 2023). Retrieved from https://www.nia.nih.gov/health/alzheimers-disease-fact-sheet

Alzheimer, A. J. Z. N. P. (1907). Uber eine eigenartige Erkrankung der Hirnrinde. *18*, 177-179.

Brownlee, J. (2019). *Generative adversarial networks with python: deep learning generative models for image synthesis and image translation*: Machine Learning Mastery.

Cassani, R., Falk, T. H., Fraga, F. J., Cecchi, M., Moore, D. K., Anghinah, R. J. B. S. P., & Control. (2017). Towards automated electroencephalography-based Alzheimer's disease diagnosis using portable low-density devices. *33*, 261-271.

Dening, T., & Sandilyan, M. B. J. N. S. (2015). Dementia: definitions and types. *29*(37), 37.

Dubois, B., Hampel, H., Feldman, H. H., Scheltens, P., Aisen, P., Andrieu, S., . . . Dementia. (2016). Preclinical Alzheimer's disease: definition, natural history, and diagnostic criteria. *12*(3), 292-323.

Fouladi, S., Safaei, A. A., Mammone, N., Ghaderi, F., & Ebadi, M. J. C. C. (2022). Efficient deep neural networks for classification of alzheimer's disease and mild cognitive impairment from scalp EEG recordings. *14*(4), 1247-1268.

Goodfellow, I., Pouget-Abadie, J., Mirza, M., Xu, B., Warde-Farley, D., Ozair, S., . . . Bengio, Y. J. A. i. n. i. p. s. (2014). Generative adversarial nets. *27*.

Gramfort, A., Luessi, M., Larson, E., Engemann, D. A., Strohmeier, D., Brodbeck, C., . . . Hämäläinen, M. S. J. N. (2014). MNE software for processing MEG and EEG data. *86*, 446-460.

Guo, J.-Y., Cai, Q., An, J.-P., Chen, P.-Y., Ma, C., Wan, J.-H., . . . Applications, i. (2022). A Transformer based neural network for emotion recognition and visualizations of crucial EEG channels. *603*, 127700.

Hochreiter, S., & Schmidhuber, J. J. N. c. (1997). Long short-term memory. *9*(8), 1735-1780.

Hochreiter, S. J. I. J. o. U., Fuzziness, & Systems, K.-B. (1998). The vanishing gradient problem during learning recurrent neural nets and problem solutions. *6*(02), 107-116.

Ieracitano, C., Mammone, N., Hussain, A., & Morabito, F. C. (2020a). *A Convolutional Neural Network based self-learning approach for classifying neurodegenerative states from EEG signals in dementia.* Paper presented at the 2020 International Joint Conference on Neural Networks (IJCNN).

Ieracitano, C., Mammone, N., Hussain, A., & Morabito, F. C. J. N. N. (2020b). A novel multi-modal machine learning based approach for automatic classification of EEG recordings in dementia. *123*, 176-190.

Jeong, J. J. C. n. (2004). EEG dynamics in patients with Alzheimer's disease. *115*(7), 1490-1505.

Johnson, K. A., Fox, N. C., Sperling, R. A., & Klunk, W. E. J. C. S. H. p. i. m. (2012). Brain imaging in Alzheimer disease. *2*(4), a006213.

Jonker, C., Launer, L. J., Hooijer, C., & Lindeboom, J. J. J. o. t. A. G. S. (1996). Memory complaints and memory impairment in older individuals. *44*(1), 44-49.

Kruse, R., Mostaghim, S., Borgelt, C., Braune, C., & Steinbrecher, M. (2022). Multi-layer perceptrons. In *Computational Intelligence: A Methodological Introduction* (pp. 53-124): Springer.

Li, Z., Liu, F., Yang, W., Peng, S., Zhou, J. J. I. t. o. n. n., & systems, l. (2021). A survey of convolutional neural networks: analysis, applications, and prospects.

Maharana, K., Mondal, S., & Nemade, B. J. G. T. P. (2022). A review: Data pre-processing and data augmentation techniques.

Malek, N., Baker, M., Mann, C., & Greene, J. J. A. N. S. (2017). Electroencephalographic markers in dementia. *135*(4), 388-393.

Marcus, C., Mena, E., & Subramaniam, R. M. J. C. n. m. (2014). Brain PET in the diagnosis of Alzheimer's disease. *39*(10), e413.

Matthews, B. W. J. B. e. B. A.-P. S. (1975). Comparison of the predicted and observed secondary structure of T4 phage lysozyme. *405*(2), 442-451.

Mattson, M. P. J. N. (2004). Pathways towards and away from Alzheimer's disease. *430*(7000), 631-639.

Medsker, L. R., Jain, L. J. D., & Applications. (2001). Recurrent neural networks. *5*, 64-67.

Morabito, F. C., Campolo, M., Ieracitano, C., Ebadi, J. M., Bonanno, L., Bramanti, A., . . . Bramanti, P. (2016). *Deep convolutional neural networks for classification of mild cognitive impaired and Alzheimer's disease patients from scalp EEG recordings.* Paper presented at the 2016 IEEE 2nd International Forum on Research and Technologies for Society and Industry Leveraging a better tomorrow (RTSI).

O'Shea, K., & Nash, R. J. a. p. a. (2015). An introduction to convolutional neural networks.

Obeid, I., & Picone, J. J. F. i. n. (2016). The temple university hospital EEG data corpus. *10*, 196.

Ogawa, S., Lee, T. M., Nayak, A. S., & Glynn, P. J. M. r. i. m. (1990). Oxygenation-sensitive contrast in magnetic resonance image of rodent brain at high magnetic fields. *14*(1), 68-78.

Rabbito, A., Dulewicz, M., Kulczyńska-Przybik, A., & Mroczko, B. J. I. j. o. m. s. (2020). Biochemical markers in Alzheimer's disease. *21*(6), 1989.

Raschka, S. J. a. p. a. (2014). An overview of general performance metrics of binary classifier systems.

Refaeilzadeh, P., Tang, L., & Liu, H. J. E. o. d. s. (2009). Cross-validation. *5*, 532-538.

Rice, D. M., Buchsbaum, M. S., Starr, A., Auslander, L., Hagman, J., & Evans, W. J. J. J. o. g. (1990). Abnormal EEG slow activity in left temporal areas in senile dementia of the Alzheimer type. *45*(4), M145-M151.

Rodrigues, P. M., Teixeira, J. P., Garrett, C., Alves, D., & Freitas, D. J. P. C. S. (2016). Alzheimer's Early Prediction with Electroencephalogram. *100*, 865-871.

Sanei, S., & Chambers, J. A. (2013). *EEG signal processing*: John Wiley & Sons.

Scheltens, P., Blennow, K., Breteler, M. M., De Strooper, B., Frisoni, G. B., Salloway, S., & Van der Flier, W. M. J. T. L. (2016). Alzheimer's disease. *388*(10043), 505-517.

Scheltens, P., Fox, N., Barkhof, F., & De Carli, C. J. T. L. N. (2002). Structural magnetic resonance imaging in the practical assessment of dementia: beyond exclusion. *1*(1), 13-21.

Simonyan, K., & Zisserman, A. J. a. p. a. (2014). Very deep convolutional networks for large-scale image recognition.

Stages of Alzheimer's. (Feb 08,2023). Retrieved from https://www.alz.org/alzheimers-dementia/stages

Stern, J. M. (2005). *Atlas of EEG patterns*: Lippincott Williams & Wilkins.

Sun, J., Xie, J., & Zhou, H. (2021). *EEG classification with transformer-based models.* Paper presented at the 2021 IEEE 3rd Global Conference on Life Sciences and Technologies (LifeTech).

Sunderland, T., Hampel, H., Takeda, M., Putnam, K. T., Cohen, R. M. J. J. o. g. p., & neurology. (2006). Biomarkers in the diagnosis of Alzheimer's disease: are we ready? , *19*(3), 172-179.

Tay, Y., Dehghani, M., Bahri, D., & Metzler, D. J. A. C. S. (2022). Efficient transformers: A survey. *55*(6), 1-28.

van Oostveen, W. M., & de Lange, E. J. I. J. o. M. S. (2021). Imaging techniques in Alzheimer's disease: A review of applications in early diagnosis and longitudinal monitoring. *22*(4), 2110.

Vaswani, A., Shazeer, N., Parmar, N., Uszkoreit, J., Jones, L., Gomez, A. N., . . . Polosukhin, I. J. A. i. n. i. p. s. (2017). Attention is all you need. *30*.

Vo, K., Vishwanath, M., Srinivasan, R., Dutt, N., & Cao, H. (2022). *Composing Graphical Models with Generative Adversarial Networks for EEG Signal Modeling.* Paper presented at the ICASSP 2022-2022 IEEE International Conference on Acoustics, Speech and Signal Processing (ICASSP).

Wang, Z., Wang, Y., Hu, C., Yin, Z., & Song, Y. J. I. S. J. (2022). Transformers for EEG-based emotion recognition: A hierarchical spatial information learning model. *22*(5), 4359-4368.

Weiner, M. J. T. j. o. n., health, & aging. (2009). Imaging and biomarkers will be used for detection and monitoring progression of early Alzheimer's disease. *13*(4), 332.

Xu, B., Wang, N., Chen, T., & Li, M. J. a. p. a. (2015). Empirical evaluation of rectified activations in convolutional network.

Yu, Y., Si, X., Hu, C., & Zhang, J. J. N. c. (2019). A review of recurrent neural networks: LSTM cells and network architectures. *31*(7), 1235-1270.